Physiochemical Characteristics, Provenance, and Dynamics of Sand Dunes in the Arid Hexi Corridor

Bing-Qi Zhu[1]*, Jia-Xing Zhang[1,2] and Chun Sun[1,2]

[1]Key Laboratory of Water Cycle and Related Land Surface Processes, Institute of Geographic Sciences and Natural Resources Research, Chinese Academy of Sciences, Beijing, China, [2]University of Chinese Academy of Sciences, Beijing, China

Dynamic changes of aeolian landforms under changing environments in a middle-latitude desert belt is a typical problem of climate change and related landscape response. It need a comprehensive understanding of the formation mechanisms of dune landforms with the supply of material suitable for aeolian transport and favorable conditions of sediment availability and wind regimes in the region. Based on comprehensive evidences from geomorphological, sedimentological, geochemical, and hydrological analysis, this study discussed the dynamical changes of different dune landforms during the past half century and their provenance in the Hexi Corridor, China. The results show that there are two states of sand dunes movement in the Hexi Corridor in the past half century, dynamic migration and basically stable. The crescent-shaped dunes move the fastest, followed by the chains of barchan dunes. Only the top of the pyramid dunes wigwags, while the parabolic dunes and the longitudinal dunes hardly move forward. The moving speed of sand dunes is positively correlated with the wind speed ≥5 m/s at a yearly scale. The grain size of sand dunes in the western Hexi Corridor is coarser than that in the central-eastern part, and also larger than those in other deserts of northern China and of the world. Different motion modes of saltation, suspension, and creeping are identified between aeolian, alluvial/fluvial and gobi sediments. Dune sands are mainly "sediments of *in-situ* rising" that originated from alluvial/fluvial/lacustrine deposits of ancient rivers, lakes, and aeolian deposits in the erosion zone of the forelands of the Qilian and Beishan Mountains and the north-neighboring deserts. This reveals a significance interaction between wind and water dynamics in the formation and evolution of aeolian landforms in the arid study area. Sufficient transport capacity is evidenced for both the western and eastern parts of the Hexi Corridor, sufficient sand supply and sand availability, however, is the favorable factor for dune formation in the east part but is the limiting factor for the west.

Keywords: sand dunes and gobi sediments, geomorphological dynamics, grain size sedimentology, major- and trace-elements geochemistry, sediment provenance, desertification, Hexi Corridor, middle-latitude desert

INTRODUCTION

The mid-latitude desert belt refers to the desert zone ranging between 30 and 60 °N latitude outside the control of the subtropical high climate in the Northern Hemisphere, more than 90% of which are distributed in the arid inland of central Asia and northern China. In northern China, about 566,000 square kilometers of land area are covered by aeolian sand, covering a wide range of

geomorphological and tectonic backgrounds ranging from 155 m below sea level to 5,000 m above sea level (Yang, 2006). The desert landscapes dominated by active sand dunes are mainly distributed in the arid areas with an average annual precipitation of less than 200 mm, while the sandy-land landscapes dominated by semi-active dunes and vegetated dunes mainly appeared in the semi-arid areas with an average annual precipitation of 200–400 mm (Zhu et al., 1980). The present geomorphology of these sandy deserts is the product of long-term and short-term changes of the interaction between endogenic forces (such as tectonic movement) and external forces (such as climate) of the earth system (Goudie, 2002; Lancaster et al., 2013; Williams, 2014; Lancaster et al., 2016; Yang et al., 2019). In turn, these deserts may have affected the global climate system indirectly through desert sediment circulation such as dust cycles (Goudie, 2002; Yang, 2006). Therefore, the understanding of desert landscape evolution will increase our understanding of the earth system.

The movement of aeolian materials and the dynamics of dune landforms are the results of the transportation and accumulation of sandy sediments under the influence of climate (especially wind and atmospheric circulation), which is the direct cause of landsurface desertification (Zhu et al., 1980; Zhu and Wang, 1992; Yang et al., 2004, Yang et al., 2012, Yang et al., 2019). Thus, in terms of genetic mechanism, formation of aeolian deposits depends on an array of requirements: the supply of material suitable for aeolian transport and favorable conditions of sediment availability and wind strength (Kocurek and Lancaster, 1999; Yang et al., 2012; Nottebaum et al., 2015b; Lv et al., 2018). In brief, the sedimentological environment (such as the supply and availability of source materials), geomorphic conditions (such as the route and distance between a specific sediment and its potential source area), and climatic conditions (such as wind regime and effective moisture controlling dust-trapping vegetation covers) constitute a complex system of dune landform development (Kocurek and Lancaster, 1999). Dune formation and dynamics in China were qualitatively or semi-quantitatively described in most early studies (Yang, 2006). Some pioneer scholars have studied the development and movement of sand dunes in the Taklamakan Desert of China, the second largest active sand desert in the world, and they quantitatively analyzed the moving speed and evolution process of local crescent dunes (Zhu et al., 1964; Zhu et al., 1980, Zhu et al., 1981a). These studies laid a solid foundation for the later development of refined and quantitative researches due to the progress of research methods and technical tools, and until now, they are still a milestone and cornerstone of desert researches in China.

The Hexi Corridor is located in the center of the desert belt in northern China and at the middle-latitudes of Northern Hemisphere (NH). It was once one of the most important trunk sections of the world-famous Silk Road, and a place where several ancient cultures converged. Today the Hexi Corridor is facing severe problems of desertification and climate change under global warming. For nearly half a century, frequent sandstorms in northern China have been considered to be the direct consequence of desertification in the Hexi Corridor, because the Hexi area is regarded as the main source area and the engine area of sandstorms in northern China (Zhang and Ren, 2003; Pu, 2005; Li and Zhang, 2007). Therefore, the problem of desertification in the Hexi Corridor is one of the major problems that have been urgently needed to be resolved in northern China for half a century.

For nearly half a century, desertification in the arid areas of northern China and its origin, causes, processes, impacts on climate change and methods of combating desertification have been studied and discussed in more detail, such as the classification (Zhu et al., 1980; Zhu et al., 1981b), causes (Wu et al., 1997; Wu and Ci, 1998; Sun, 2000; Sun and Li, 2002; Wu and Ci, 2002; Runnstrom, 2003), trends (Zhu, 1985; Ci et al., 2002; Wang et al., 2004; T. Wang et al., 2003, Wang et al., 2004a, Wang et al., 2004b) and environmental effects (Ci and Yang, 2004; Yang et al., 2008) of desertification in China. Although significant progress has been made in the study of desertification in China in recent decades and the understanding of the classification of desertification has reached a basic consensus, its causes are still controversial. Many scientists believe that the desertification in northern China is mainly caused by human activities (Wu, 2001; Wang et al., 2003a; Wang et al., 2004b), while others believe that climate change is the main cause of desertification in northern China (Zhao, 1981; Wang, 2002; Han, 2003; Wang et al., 2005, Wang et al., 2006a, Wang et al., 2008a). But in any case, desertification is a dynamic process, which is potentially affected by surface erodibility and atmospheric erosivity (Thomas et al., 2005; Thomas and Leason, 2005) and may also be affected by geomorphological processes on the geological time scale even greater than the effects of climate change (Nottebaum et al., 2015a), and these dynamics are still not well understood at present, especially at the inter-decadal time scale.

The purpose of this study is, based on the comprehensive evidences from the extensive dune geomorphological survey, the sedimentological and geochemical analysis of dune sediments to understand the provenance and dynamic changes of sand dunes in the Hexi Corridor and their formation mechanism during the past half century.

BACKGROUND AND ANALYTICAL METHODS

Natural Backgrounds of the Hexi Corridor

The Hexi Corridor is geographically located in the central and western parts of Gansu Province in Northwest China (**Figures 1**, **2**), including Wuwei, Jinchang, Zhangye, Jiuquan, Jiayuguan and other cities in the west of the Yellow River, with a total area of approximately 5,100 square kilometers.

In terms of geomorphology, the Hexi Corridor represents the transition zone from high mountain areas towards the lower northwestern Chinese deserts, located in the lowland area between the Qilian Mountains to the south and the Alashan Plateau to the north (**Figure 2**). The Alashan Plateau distributes three large sandy deserts of China, i.e., the Badanjilin Desert, the Tenggeli Desert and the Ulanbuhe Desert. The Qilian Mountains is trending west-northwest-east-southeast (WNW-ESE) and
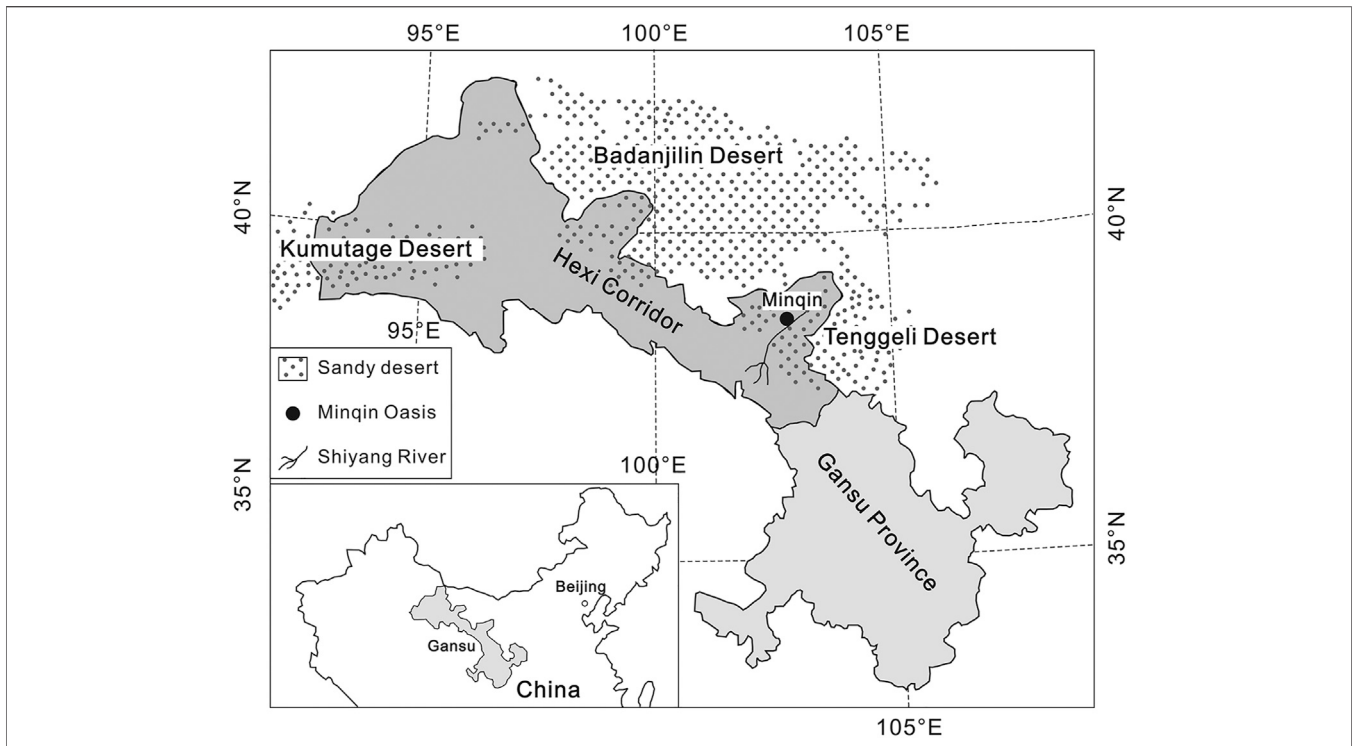
FIGURE 1 | Geographical position of the Hexi Corridor in China (the Hexi Corridor is located in the west of Gansu Province and is a part of Gansu Province).
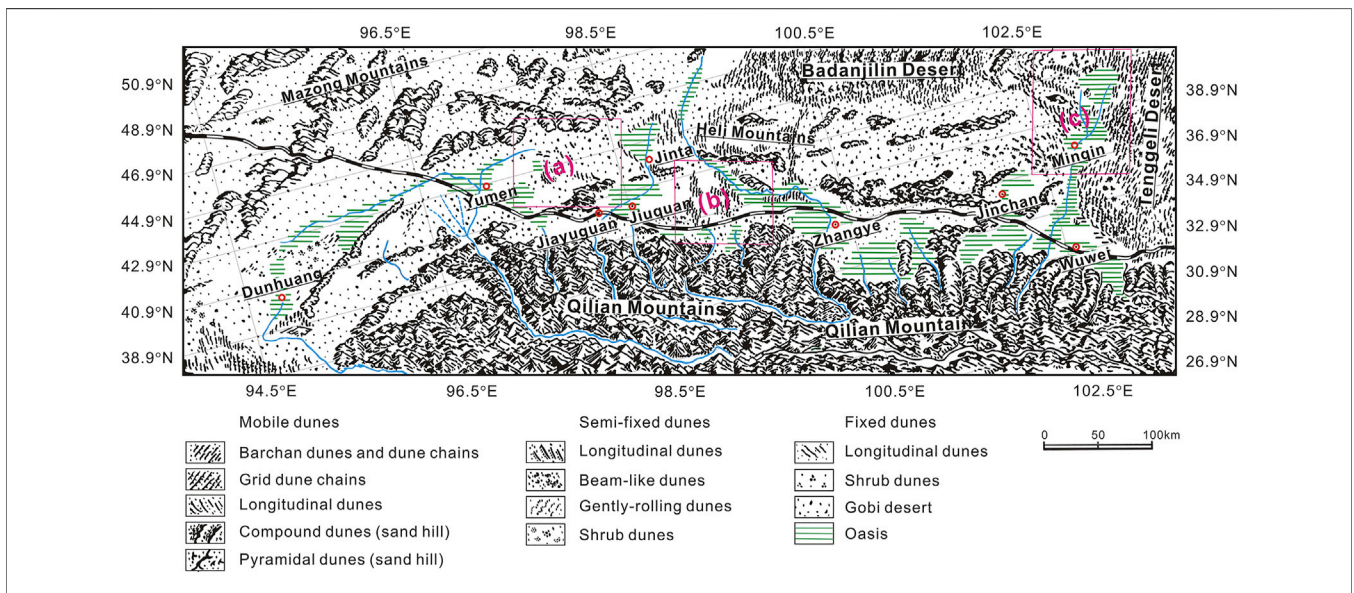
FIGURE 2 | Geomorphological map of the Hexi Corridor (modified after Wang (2003)).

reaches up to 5,700 m above sea level (a.s.l.). It was uplifted during the Caledonian orogenesis and got reactivated by the India-Eurasia collision during Cretaceous and Neogene times (Tapponnier et al., 1990; Meyer et al., 1998). It dominantly consists of metamorphic and sedimentary rocks,

i.e., sandstones and conglomerates (Bureau of Geology and Mineralogy Resources of Gansu Province (BGMRGP), 1984).

The geomorphologic landscape appearance is remarkably different in the western part compared to the central and eastern parts of the Hexi Corridor. The west is mainly

dominated by gravel gobi surfaces, accompanied by rare sand sheets and dune fields in the surrounding of the Huahai palaeolake (G. Wang et al., 2003, N. Wang et al., 2013), while the central and east exhibit frequent alternation of alluvial and lacustrine deposits, several dune fields, sand sheets, and widespread oases including cropland (Nottebaum et al., 2015a).

In climate, the Hexi Corridor is situated in the center part of the temperate desert belt in the mid-latitudes of Northern Hemisphere. Except for the forest and grasslands distributed in the middle- and high-elevation mountain areas in the south, most of the Hexi Corridor is under a typical arid climate with desert landforms widely developed. The desert types are dominated by gobi desert and sandy desert, which account for 46.64% of the total area of the region.

In hydrology, the melting water of ice and snow in the high Qilian Mountains in the south converges into several large rivers flowing northward into the Hexi Corridor, including the Shule River, the Heihe River, and the Shiyang River from west to eat (**Figure 2**). In the middle and lower reaches of these rivers flowing through the corridor from south to north, diluvial and alluvial fans are well developed, and hydrologically, they are also the main locations of spring overflow zone of each catchment derived from the Qilan Mountains. Oases are widely developed in the toes of these alluvial fans and are the major agricultural exploitation areas and the resident agglomeration areas of northwest China. The ephemeral drainages of the western Hexi Corridor terminate close to the southern edge of the adjacent Beishan Mountains to the north which was the terminal basin hosting Huahai palaeolake (**Figure 2**), whereas the main eastern drainage (Heihe River) flows farther north into the Ejina basin, feeding the Juyanze, Sugunur, and Garshunnur palaeolakes (Hartmann and Wünnemann, 2009).

In sedimentological geology, the Hexi Corridor was affected by widespread Quaternary (glacio-) fluvial sediment accumulation (Hetzel et al., 2004; Kuster et al., 2006), resulting in several generations of alluvial fans. These fans are partly affected by tectonic activity (Hetzel et al., 2002) and subsequently dissected by fluvial incision. Due to the geomorphological differences between the western and central eastern parts of the Hexi Corridor, their surface strata also have two different sedimentary characteristics. One is that the gravel strata are often covered by interbedded sedimentary strata of aeolian and alluvial/proluvial sediments, and the other is that the aeolian strata in sand dunes are often interrupted by flood deposition. Geochronology and paleoenvironment studies from the superficial sedimentary strata indicate that there is also a completely different sedimentary evolution history between the western and central-eastern parts of the Hexi corridor during the Late Quaternary (Nottebaum et al., 2015a). For example, the sedimentary process in the western part of the Hexi Corridor is limited to a short period of the Pleistocene-Holocene transition, while the sedimentary process in the central-eastern of the Corridor occurs throughout the Holocene, reflecting a history of frequent sediment recycling during the Holocene.

Aeolian sediments (loess, loess-like, sand and dust) and dune landforms are widespread in the western, central and eastern parts of the Hexi Corridor (Zhang et al., 2008; Nottebaum et al., 2014, Nottebaum et al., 2015b). In terms of aeolian landforms, sand dunes or dune fields in the Hexi Corridor are mainly distributed in a narrow and long belt between the Qilian Mountains and the Heli mountains from the west of Wushaoling to the east of Palaeo-Yumenguan (**Figure 2**) (Zhu et al., 1980). Compared with dune landforms in the adjacent areas of the Badanjilin and Tenggeli Deserts, in which the sand dunes tend to be convergent in spatial distribution, while the Hexi Corridor is different, where the dunes are almost scattered, mainly distributed in the vicinity of oases along some rivers, in the oasis or gobi desert areas (**Figure 2**). From east to west in the dune belt, sand dunes are mainly distributed around the Minqin Oasis in the lower reaches of the Shiyang River, the Zhangye and Gaotai oases in the middle reaches of Heihe River, the Jiuquan and Jinta oases in the lower reaches of the Beidahe River, and the Dunhuang oasis in the lower reaches of the Danghe River (**Figure 2**) (Zhu et al., 1980).

The total area of dune fields in the Hexi Corridor is about 754 square kilometers, and many big crescent-shaped dunes and chains of crescent-shaped dunes develop on the edges of oases. The Minqin Basin is a typical area with dune landforms development in the Hexi Corridor. It is located at the lower reaches of the Shiyang River and the western edge of the Tenggeli Desert. The annual average precipitation is about 116.4 mm and the annual average wind speed is about 2.25 m/s. A large number of crescent-shaped dunes are distributed on the northwestern edge of the oasis, i.e., the windward of sand-transport winds in the oasis.

Historically, the Hexi Corridor was a necessary place for the famous ancient Silk Road in China. In modern times, however, the expansion of population and socio-economic development of the Hexi Corridor, as well as the human-caused competitive redistribution of water resources, have led to the onset and enhancement of desertification in the Hexi Corridor (Pu, 2005). The expansions of sand dunes and dune fields in the corridor, and even the combination with surrounding sandy desert, have occurred in the past 2 ka (Zhu and Wang, 1992; Ren et al., 2014).

Methods and Analytical Data

Formation and characteristics of dune landforms are considered to be the result of a complex interplay between sediment properties and local preconditions (Nottebaum et al., 2015b). Although wind regime, surface condition, and sediment availability all control sand dune formation (Pye, 1995; Kocurek and Lancaster, 1999), geoscientists have mostly put emphasis on the wind regime. However, researches show that the formation of dune cannot be explained solely on wind because different dune types can form under the same wind regime in a given area (Rubin and Hesp, 2009; Lv et al., 2018). For example, in areas with little or no vegetation, dune formation depends strongly on wind regime and sediment availability (Wasson and Hyde, 1983; Baas and Nield, 2007), and both factors must be considered in studies on the formation and morphology of aeolian dunes; otherwise, modern dune morphology may lead to erroneous interpretations of the evolutionary history of dune

environments (Rubin and Hesp, 2009). Therefore, sediment properties and local preconditions must be paid attention to.

In detail, sediment properties are partly inherited from source materials, e.g., grain size and geochemical/mineralogical composition (e.g., Jahn et al., 2001; Prins and Vriend, 2007; Feng et al., 2011; Guan et al., 2013; Vandenberghe, 2013; Nottebaum et al., 2014, Nottebaum et al., 2015b). Important local preconditions comprise surface and topographic properties, e.g., the geomorphologic setting, vegetation cover, and surface roughness on various spatial scales (Mason et al., 1999; Hugenholtz and Wolfe, 2010; Stauch et al., 2012; Stauch et al., 2014; Nottebaum et al., 2014, Nottebaum et al., 2015b) and wind conditions (e.g., Pye, 1995; Lu et al., 2000; Sun et al., 2003; Kimura et al., 2009). Thus, an insight into the potential relationship between dune-forming factors related to the wind regime, surface conditions and the available sediment sources within a dune system is needed.

Based on this idea, in this study, our analysis methods and data mainly focus on the following aspects of dune landform: first, the data of morphological parameters varied with time in different dune types and dune units and the related acquisition method of these data are used to explore the characteristics of dynamic change and evolution of dune landforms in the study area. Secondly, the grain-size sedimentological data of sand dunes and their analytical methods are used to explore the characteristics of particles' mixing, potential transport mode and sedimentary maturity of aeolian sand in the study area, and to provide sedimentological clues about the wind forcing intensity and source area distance of dune sediments. Thirdly, the geochemical data and related analytical methods of dune sediments are used to determine the material sources of these detrital sediments in the study area. Fourthly, the meteorological, hydrological, and climatic data of dune fields and the surrounding areas are used to explore the relationship between the dynamic evolution of dune landforms and environmental factors and its implications on desertification in the study area. These data and related analysis methods are described in detail below.

For the data of dune geomorphology, the first method is to use the sample-quadrate survey procedure to measure the height and shape of typical high dunes in the field with a rangefinder, and the second is to measure the length, angle and width of the windward slope and downwind slope of each dune in the sample quadrate and between different quadrates along the local dominant wind direction by using rangefinder and remote sensing image scales (such as Google Earth scales, etc.), and then the comprehensive geomorphic data of sand dunes in the region is obtained. In addition to the geomorphological data of sand dunes themselves, landscape researchers will also use the sample-quadrate survey method to investigate the ecological parameters of vegetation cover in the selected sampling area. For both geomorphological and ecological surveys, sub-scale sample quadrates will be selected from the upper, middle, and lower parts of the windward and leeward slopes of each dune. Three quadrates can be selected from the dune slope in the windward and downwind directions of each dune along the local prevailing wind direction and the size of each quadrate can be designed as 5 m × 5 m or smaller. In recent years, observation works have

been carried out in different parts of the Hexi Corridor to investigate the different landform types of widespread sand dunes at a geomorphic unit scale in the field (Chang et al., 2016, Chang et al., 2017; Lang et al., 2017), including the crescent-shaped (barchan) dunes, chains of barchan dunes, pyramid-shaped dunes, parabolic dunes, and longitudinal dunes belt. Based on time-series satellite remote sensing image data in different periods, the geomorphological parameters of these dunes are also obtained (Zhang and Dong, 2014; Chang et al., 2016, Chang et al., 2017; Lang et al., 2017). In this study, the observation data and digital data were collected and sorted out systematically and corrected uniformly. Parts of these comprehensive data of geomorphological parameters of sand dunes in the Hexi Corridor are shown in **Tables 1**, **2**. In addition to the above-mentioned intuitive survey and measurement of geomorphic parameter of sand dunes, quantifying the structure of wind-blown sand flow and the movement rate of dunes is also the most direct and effective means to explain the dynamic change of dunes and their geomorphological evolution (Dong et al., 1998; Chen and Liu, 2011; He et al., 2012; Dong and Huang, 2013; J. Wang et al., 2013; Hu et al., 2016; Mao et al., 2016). Generally, there are two methods to study the moving velocity of sand dunes, one is early positioning observation (Minqin Desert Control Experiment Station (MDCES), 1975; Dong et al., 1998; He et al., 2012; Shi et al., 2018) and the other is based on remote sensing images (Chen and Liu, 2011; Dong and Huang, 2013; Mao et al., 2016). Research works based on the both methods have been carried out in dune fields of the Hexi Corridor (Minqin Desert Control Experiment Station (MDCES), 1975; Chen and Liu, 2011; Chang et al., 2015, Chang et al., 2016, Chang et al., 2017; Hu et al., 2016; Shi et al., 2018). On this basis, this study integrates and organizes the different observation data of dune movement measurement in the Hexi Corridor. Parts of these data of dune movement measurement are shown in **Table 3**. The specific analysis methods mentioned above are as follows.

Based on comprehensive investigations of the crescent-shaped dunes and the chains of crescent-shaped dunes at the edge of the Minqin oasis in the Hexi Corridor, several typical crescent-shaped dunes were selected for field observation of sand flow, wind erosion and sand deposition. The specific methods of observation are stated here taken two typical dunes as examples. Two tall crescent-shaped dunes (dunes No. 1 and No. 2) were selected in Xishawo (the western edge of the Tengerli Desert) in Minqin and several automatic observation recorders of wind speed and wind direction were set up in key parts of the dunes. For wind speed observation, the observation period for dune No. 1 was from April to September 2014, when the highest point of this dune was separated from the dune ridge line at the beginning of the observation. The observation period of dune No. 2 was from April to September 2015, when the highest point of the dune was coincident with the dune ridge line at the beginning of the observation. While observing the wind speed and wind direction, several wind erosion rods were set up at each key part of the sand dunes to measure the wind erosion depth and the sand deposition thickness of each part. At the same time the vegetation and potential sand source conditions around the

TABLE 1 | The locations, heights, movement directions, and lengths of dunes in the Hexi Corridor.

Dune type	Dune ID	Geographic location		Height of dunes (m)	Movement direction (N-W)	Length of the slopes (m)		Source
		Longitude (E)	Latitude (N)			Upwind	Downwind	
Barchan dunes	1	102°55′16″	38°37′52″	9.8	48°	438.5	252	Chang et al. (2016), Chang et al. (2017)
	2	102°55′13″	38°38′00″	11.2	48	163.3	492.7	Chang et al. (2016), Chang et al. (2017)
	3	102°55′05″	38°36′06″	9.5	48°	129.2	163.3	Chang et al. (2016), Chang et al. (2017)
	4	102°55′02″	38°37′51″	3.7	48°	304.2	484.1	Chang et al. (2016), Chang et al. (2017)
	5	102°56′34″	38°32′11″	7.9	45°	271.7	229.4	Chang et al. (2016), Chang et al. (2017)
	6	102°56′43″	38°31′59″	7.6	46°	762.3	430.1	Chang et al. (2016), Chang et al. (2017)
	7	102°54′37″	38°25′47″	3.9	45°	295.9	80.8	Chang et al. (2016), Chang et al. (2017)
	8	102°52′56″	38°25′17″	5.9	87°	42.6	52	Chang et al. (2016), Chang et al. (2017)
	9	98°49′44″	39°57′41″	5	51°	350.4	254.5	Chang et al. (2016), Chang et al. (2017)
	10	98°49′59″	39°58′07″	2.6	54°	222.8	437.9	Chang et al. (2016), Chang et al. (2017)
	11	98°49′18″	40°00′41″	7.2	57°	184.6	197.3	Chang et al. (2016), Chang et al. (2017)
Chains of barchans dunes	12	102°54′53″	38°37′46″	6.4	54°	726.9	752.8	Chang et al. (2016), Chang et al. (2017)
	13	102°55′55″	38°37′48″	5.8	54°	443.4	406.7	Chang et al. (2016), Chang et al. (2017)
	14	102°54′46″	38°37′24″	11.1	50°	794.8	658.4	Chang et al. (2016), Chang et al. (2017)
	15	98°51′17″	39°57′59″	13.8	53°	413.6	361.1	Chang et al. (2016), Chang et al. (2017)
	16	98°51′31″	39°57′31″	8.7	54°	501.8	466.2	Chang et al. (2016), Chang et al. (2017)
	17	98°48′04″	39°58′50″	9.6	53°	554	445	Chang et al. (2016), Chang et al. (2017)
Pyramid dunes	18	94°42′23″	40°05′16″	25.8	SW-NE	—	—	Chang et al. (2016), Chang et al. (2017)
	19	94°42′10″	40°05′14″	90.3	SW-NE	—	—	Chang et al. (2016), Chang et al. (2017)
	20	94°41′47″	40°05′11″	76.6	SW-NE	—	—	Chang et al. (2016), Chang et al. (2017)
	21	94°40′53″	40°05′11″	121.8	SW-NE	—	—	Chang et al. (2016), Chang et al. (2017)
	22	94°40′43″	40°05′09″	114.1	SW-NE	—	—	Chang et al. (2016), Chang et al. (2017)
	23	94°40′12″	40°05′24″	88.9	SW-NE	—	—	Chang et al. (2016), Chang et al. (2017)
Parabolic dunes	24	102°57′15″	38°36′27″	4.6	—	286.1	35.3	Chang et al. (2016), Chang et al. (2017)
	25	102°57′42″	38°36′26″	4.4	—	228.9	188	Chang et al. (2016), Chang et al. (2017)
	26	102°58′15″	38°36′10″	3.3	—	133.3	198.5	Chang et al. (2016), Chang et al. (2017)
	27	93°59′40″	38°37′08″	3.7	—	396	302.2	Chang et al. (2016), Chang et al. (2017)
	28	98°41′36″	41°35′64″	4.4	—	59.9	0	Chang et al. (2016), Chang et al. (2017)
	29	98°41′20″	40°08′51″	4.1	—	15.7	17.7	Chang et al. (2016), Chang et al. (2017)

TABLE 1 | (*Continued*) The locations, heights, movement directions, and lengths of dunes in the Hexi Corridor.

Dune type	Dune ID	Geographic location		Height of dunes (m)	Movement direction (N-W)	Length of the slopes (m)		Source
		Longitude (E)	Latitude (N)			Upwind	Downwind	
Accumulated sand-belts (longitudinal dunes belts)	30	103°12′36″	38°47′57″	15.2	—	70.4	Farmland	Chang et al. (2016), Chang et al. (2017)
	31	103°13′30″	38°48′36″	17.1	—	44	Farmland	Chang et al. (2016), Chang et al. (2017)
	32	103°32′03″	39°02′12″	18.6	—	811.7	Farmland	Chang et al. (2016), Chang et al. (2017)
	33	103°31′29″	39°02′10″	5.6	—	707.7	Farmland	Chang et al. (2016), Chang et al. (2017)
	34	103.29′49″	39°02′34″	12.2	—	1557.6	Farmland	Chang et al. (2016), Chang et al. (2017)
	35	103°26′19″	39°02′20″	9.4	—	207.1	223.4	Chang et al. (2016), Chang et al. (2017)

TABLE 2 | Morphological characteristics of barchans dunes in the Hexi Corridor.

Dune ID	Plots area	Height (m)	Thickness of camponotus (m)	Length (m)	Width (m)	Slope of leeward direction (°)	Forward direction (°)	Length of upwind slope (m)	Length of downwind slope (m)	Source
1	Minqin 3–1	9.8	123.3	214.6	202.5	32.6	N48°W	662.9	378	Chang et al. (2017)
2	Minqin 3–2	11.2	155.7	294.4	227.4	32.2	N48°W	163.3	491.6	Chang et al. (2017)
3	Minqin 3–3	9.5	12.5	197.5	209.8	32.1	N48°W	134.2	176.6	Chang et al. (2017)
4	Minqin L	3.7	78.8	86.5	81.8	31.8	N48°W	251.8	367.8	Chang et al. (2017)
5	Minqin 9	7.9	90.8	112.5	81.5	32.9	N45°W	214.3	253.3	Chang et al. (2017)
6	Minqin 10	7.6	86.7	136.8	64.7	31.5	N46°W	137.9	430.1	Chang et al. (2017)
7	Minqin 11	11.6	104.4	183.6	57.3	31.6	N46°W	179.9	243.1	Chang et al. (2017)
8	Minqin 12	8.6	64.1	131.4	77.9	30.1	N46°W	135.2	697.3	Chang et al. (2017)
9	Jinchang 1	8.4	130.3	197.6	123.2	31.7	N55°W	227.4	372.1	Chang et al. (2017)
10	Jingta 1	6	83.7	125.3	104.8	31.5	N63°W	250.4	129.5	Chang et al. (2017)
11	Jinta 2	5.3	73.5	104.8	76.6	31.7	N63°W	108.2	419.8	Chang et al. (2017)

observed dunes were measured. In the process of wind speed observation, the measured height of wind speed and wind direction was 50 cm from the ground, sampling once every 20 min, and statistics were made with every 2 m/s as a wind speed level. The maximum wind speed observed was 14.9 m/s. During the observation of wind erosion and sand accumulation processes, No. 8 steel wires (level 8 in thickness) were used for the observation of wind erosion depth and sand accumulation depth, with one end of the wire being buried underground and the other end being kept 30 cm above the dune surface. The height (depth) of the ground were measured for each observation. In this study, the forward wind system and the reverse wind system were defined. The forward wind refers to the local main wind direction (the NW wind), and the reverse wind is the SE

TABLE 3 | Annual movement distance and speed of sand dunes in the Hexi Corridor. Data from Shi et al. (2018).

Area or observation site	Duration (a)	Width of dune (m)	Movement distance of dune (m)	Movement speed of dune (m/a)
Gulang	8	277.95	38.4	4.8
Minqin	9	132.87	55.8	6.2
Jinchang	9	156.32	40.5	4.5
Linze	8	240.14	33.6	4.2
Gaotai	8	170.30	11.2	1.4
Jinta	9	290.70	36.0	4.0
Dunhuang	8	225.75	6.4	0.8

wind. Whether it is a forward wind process or a reverse wind process, the windward slope of a sand dune is defined in accordance with the forward wind commonly documented in the previous research practices, that is, if the local main wind direction is NW wind, the NW slope of a sand dune is considered to be the windward slope of the dune in this study. The definition of the leeward slope is the opposite of the above. The vertex of a sand dune refers to the highest point of a dune. The chord length of a dune refers to the distance between the two wing endpoints of the dune. The aspect ratio of a dune refers to the ratio of the total length to the total width of the dune. The bow back thickness of a dune refers to the distance from the bottom of the windward slope to the bottom of the leeward slope of the dune. Meteorological and climatological data were collected from local weather stations and the China Meteorological Science Data Sharing Service Network.

In order to unify the multi-parameter measurement data obtained from different research works, this paper classifies and adjusts the data of geomorphic parameters and dynamic change parameters of sand dunes in the Hexi Corridor from three aspects, taking the crescent-shaped dune at the edge of oasis in the Hexi Corridor as an example: sand dune distribution environment, sand flow in dune field and characteristics of two wings of sand dunes. Furthermore, a unified analysis was made in the aspects of wind speed classification and wind direction characterization. Among them, the forward wind was classified according to 2 m/s as a wind speed level, which was divided into five grades: <2 m/s, ≥2 – <4 m/s, ≥4 – < 6 m/s, ≥ 6–8 m/s and ≥8 m/S. The wind speed of the reverse wind was relatively small, so it was graded as a wind speed level of 1 m/s. The wind speed data analysis was completed using SPSS 13.0. The detailed results can be seen in **Tables 1–3**.

In addition to field surveys and measurements, the data of geomorphic parameters of the large-scale dune types and dune shapes of the study area are also obtained from some remote sensing image data. For example, it can be distinguished and extracted from the combination of Google Earth high-definition images and environmental disaster mitigation satellite (HJ-1A/1B Satellite) images. The environmental disaster mitigation satellite imagery is provided by the China Resources Satellite Application Center, with a resolution of 30 m. The geomorphological map produced by the environmental disaster mitigation satellite images uses colour synthesis of bands 3, 2 and 1. The range of oasis and desert is divided by the normalized vegetation index (NDVI). NDVI > 0.1 is classified as an oasis and NDVI ≤ 0.1 is classified as a desert. NDVI is calculated by using the Band 3 and Band 4 data of environmental disaster mitigation satellite images. The calculation formula is NDVI = (B2 − B1)/(B2 + B1). B1 and B2 are the Band 3 and Band 4 of satellite, respectively. The remote sensing image processing is carried out in ENVI 4.4 and the output map is from ArcMap v9.3 (ESRI).

Erodible clastic sediments as the material sources are the fundamental base for the formation of sedimentary landforms (Pettijohn et al., 1972; Taylor and McLennan, 1985). Therefore, identifying the composition, source, transport, and accumulation of wind-induced materials in an arid environment is a prerequisite for understanding the formation of dune landforms (Zhu et al., 1980; Zhu et al., 1981a; Yang et al., 2012). Although sediment sections are usually used in many studies to observe the variability of sediment accumulation and sources in one location through time, in this study, the investigation approach of surface aeolian sediment samples at a regional scale is applied. The surface sample approach allows identification of distribution pathways by considering the continuous variety of geomorphological settings (Lehmkuhl, 1997; Kuster et al., 2006; Schettler et al., 2009; Nottebaum et al., 2014; Zhu and Yu, 2014; Zhu et al., 2014; Nottebaum et al., 2015b). Therefore, this method offers an opportunity to analyze the spatial distribution and composition of surface aeolian sediments accumulated under variable conditions and from different perspectives (i.e., geomorphological setting, relief, and vegetation).

Grain size composition and distribution of aeolian sediment is an important indicator to understand the formation and development of sand dunes, because grain size distribution (GSD) analysis of sediments is an established tool to analyze the composition of sediments and to distinguish different transport, accumulation and potential remobilization processes (Folk and Ward, 1957; Friedman, 1961; Ashley, 1978; Bagnold and Barndorff-Nielsen, 1980; McLaren and Bowles, 1985; Sun et al., 2002; Qiang et al., 2007; Weltje and Prins, 2007; Qiang et al., 2010; Guan et al., 2013; Vandenberghe, 2013; Nottebaum et al., 2014; Zhu et al., 2014; Zhu and Yu, 2014). The depositional environment (aeolian, fluvial or lacustrine) and the movement types (creep, saltation or suspension) of sediments in the transportation process can be identified and distinguished by using grain size parameters of sand particles (Folk and Ward, 1957; Friedman 1961; Bagnold and Barndorff-Nielsen, 1980; McLaren and Bowles, 1985; Nottebaum et al., 2014; Zhu et al., 2014). At present, grain-size analysis of aeolian sediments and

relevant detrital sediments, such as alluvial and proluvial fans, lacustrine deposits, fluvial deposits, has been widely carried out in the Hexi Corridor (Nottebaum et al., 2014, Nottebaum et al., 2015b; Zhu et al., 2014; Zhu and Yu, 2014; Zhang and Dong, 2015; Zhang et al., 2016; Pan et al., 2019; Zhang et al., 2020). On this basis, this study systematically collects and organizes these granular data and records, which makes it possible to further conduct a comprehensive and comparative study on the dunes in the Hexi Corridor from a perspective of sedimentology. The specific analysis methods of grain size are as follows.

The grain-size sedimentological data of dune sediments from different sources used in this paper are almost measured by using the instrument of high-frequency mechanical vibrating screen (shaker), so the grain size data from different sources have good coordination and consistency, and do not need further classification and unification. The sample analysis method and data processing method of the grain size data are as follows. Different dune fields in the Hexi Corridor were widely sampled in the study region. Dune surface sediments were collected from the windward toe, stoss, crest, and leeward toe. At each site, surface materials (0–1 cm layer) from a 20 cm × 20 cm transect area were collected; each sample weighted about 0.5–1 kg. Grain size analyses of all samples were undertaken using standard sieving (on a Retsch AS200 Sieving Shaker, Haan, Germany) for 10 min. Each fraction of the sample was weighed to the nearest 0.001 g. All the granularity analysis data in this paper are uniformly calculated using the method of Folk and Ward (1957). The mass proportion of each fraction in grain size is expressed in phi (φ) unit ($\varphi = -\log_2 d$, where d is grain size in millimeters), and described using the parameters of mean size (Mz), standard deviation (δ_1), skew (Sk1), and kurtosis (KG), as proposed by Folk and Ward (1957). Characterized grain size and sorting parameters were also calculated following the formulae devised by Folk and Ward (1957).

The analysis of major and trace elements, including rare earth elements, has become a reliable technique for detecting the source of desert sediments (Muhs et al., 1995, Muhs et al., 1996; Honda and Shimizu, 1998; Pease et al., 1998; Wolfe et al., 2000; Zimbelman and Williams, 2002; Pease and Tchakerian, 2003; Muhs, 2004; Yang et al., 2007; Zhu and Yang, 2009; Jiang and Yang, 2019). The reason is that for aeolian sediments, the differences in compositions and distributions of rare earth elements and other trace elements in different samples/sub-fractions are largely controlled by the parent-rock compositions, because these elements only exist in specific minerals and are difficult to be lost during transportation (Pettijohn et al., 1972; Taylor and McLennan, 1985). In the Hexi Corridor, preliminary results have been achieved in the case studies of analyzing the elemental compositions of aeolian sediments using major- and trace-element geochemical methods (e.g., Schettler et al., 2009; Wang et al., 2010; Ren et al., 2014; Pan et al., 2019; Zhang et al., 2020), which provide basic data for this study to comprehensively identify the material sources of different dunes in the study area.

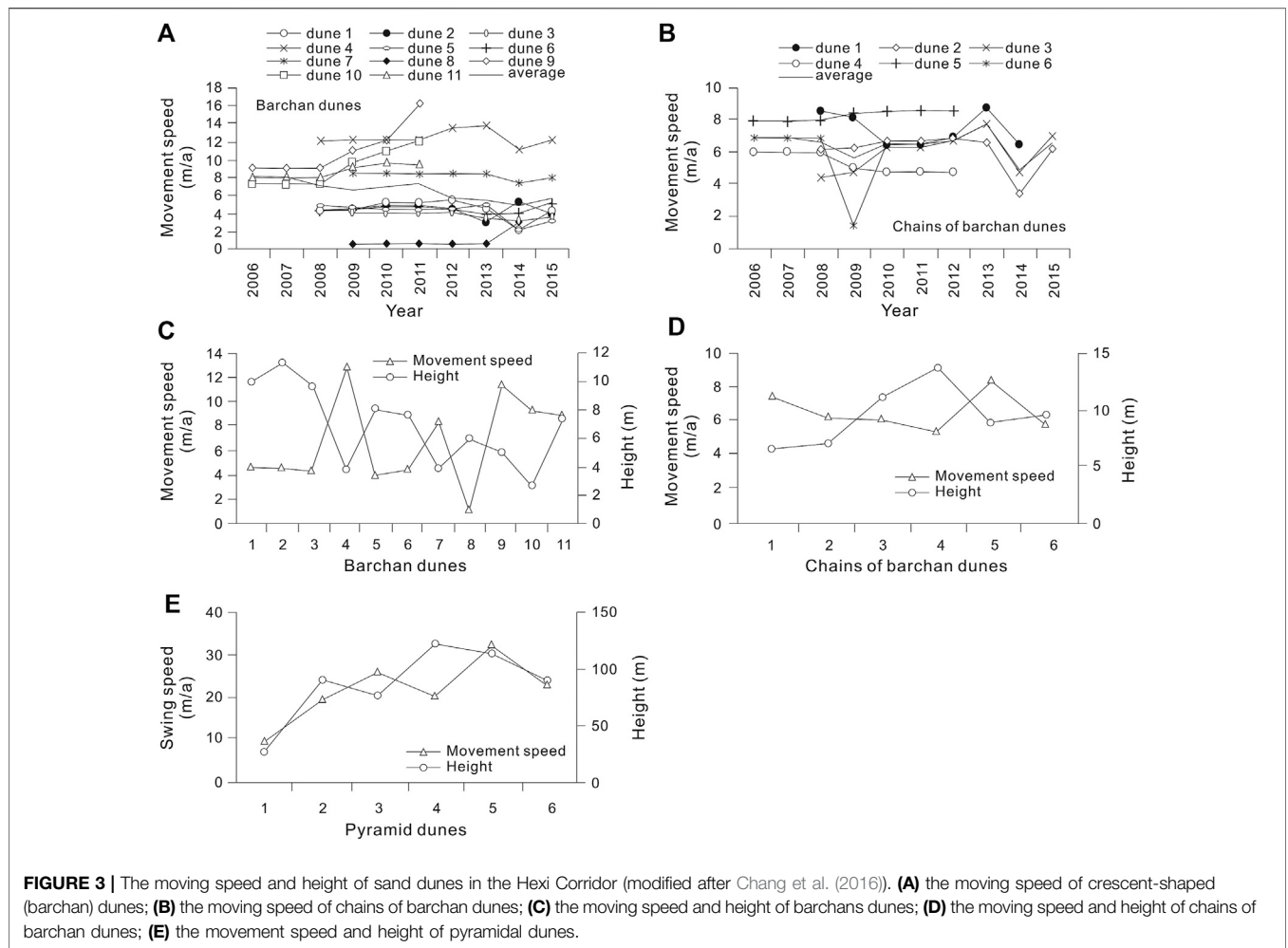The geochemical data of major and trace elements compositions of dune sediments used in this study are almost obtained by using the XRF analysis method, so the data from different sources have good coordination and consistency. The measurement method and processing method of these data are as follows. Bulk samples of dune sands from the Hexi Corridor were taken for laboratory preparation and measurements. Samples were dried at low temperature (43°C) for 72 h and grinded to less than 75 mm. Up to 4 g of sample was weighed and poured into the center of the column apparatus, together with boric acid, and pressurized to 30 t/m2 for 20 s using a YYJ-40 semiautomatic oil hydraulic apparatus. The processed samples, approximately 4 cm in diameter and 8 mm thick, were analyzed by using a Philips Panalytical Magix PW2403 X-ray fluorescence (XRF) spectroscope. Analytical results are reported in oxide compound form apart from trace elements which are given in elemental form. The standard deviations for the major elements were estimated by the repeated analysis of the samples. Standard deviations were <10% for Ce, Co, Cs, Ga, La, Rb, Sc, Y, Hf and Zr, <8% for Ba, Bi, Cr, Mn, Ni, Sr and V, <3% for MgO and Na2O and <0.5% for the other major elements. Our analysis of geochemical data focuses on element abundance and element ratio methods widely used in geochemistry. In addition, we apply hierarchical cluster analysis of the data to group samples based on multi-elements analysis (Zhu et al., 2017). Hierarchical cluster analysis, based on Ward's method (Ward, 1963) and the Euclidean distance, was conducted to classify samples using trace elements as the variables (Wolff and Parsons, 1983; Zhu and Wang, 2016). Trace elements (Ba, Bi, Ce, Co, Cr, Cs, Ga, La, Mn, Rb, Sr, V and Zr) and Ti whose average abundance were larger than 20 ppm were selected for hierarchical cluster analysis in order to avoid errors caused by the detection limit of analytical instrument. To reduce the impact of the large difference in abundance level of the various elements, the data were standardized to z scores, with a mean of 0 and a standard deviation of 1. Hierarchical cluster analysis was performed using the IBM SPSS Statistics 20 program.

The continuous data records of different meteorological parameters of local weather stations in the Hexi Corridor in the past half century, such as temperature, precipitation, relative humidity, wind speed, strong wind days and sandstorms days, will not only be the basis for this study to discuss the regional climate change under the background of global warming, but also the basis for exploring the response of regional landscape to climate change based on the statistical relationship between geomorphic parameters and climate parameters on a multi-decade time scale. Therefore, this study collects and uses the meteorological data of the Hexi Corridor for the past half a century to analyze the regional climate change and its relationship with the dynamic changes of dune landforms.

RESULTS

Geomorphological Characteristics of Sand Dunes in the Hexi Corridor

The comprehensive data on the heights of different types of sand dunes widely developed in different areas of the Hexi Corridor, as well as other geomorphic parameters of these dunes, can be found in **Tables 1**, **2** and **Figure 3**. It can be seen from **Tables 1**, **2** and
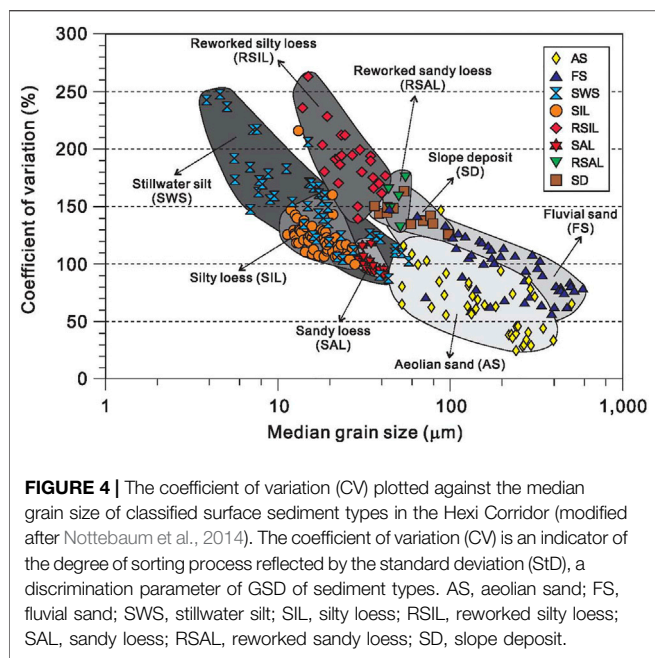
FIGURE 3 | The moving speed and height of sand dunes in the Hexi Corridor (modified after Chang et al. (2016)). **(A)** the moving speed of crescent-shaped (barchan) dunes; **(B)** the moving speed of chains of barchan dunes; **(C)** the moving speed and height of barchans dunes; **(D)** the moving speed and height of chains of barchan dunes; **(E)** the movement speed and height of pyramidal dunes.

Figure 3 that the average height of typical crescent-shape (barchan) dunes in the Hexi Corridor is about 6.75 m, the maximum is about 11.20 m, and the minimum is only about 2.60 m. The average height of typical chains of barchan dunes in the study area is about 9.23 m, the maximum is about 13.80 m, and the minimum is only about 5.80 m. The typical pyramid-shaped dunes in the study area have an average height of about 86.25 m, with a maximum of about 121.80 m and a minimum of about 25.80 m. The average height of typical parabolic dunes in the study area is about 4.08 m, the maximum is about 4.60 m, and the minimum is only about 3.38 m. The average height of typical longitudinal dunes in the study area is about 13.02 m, the maximum is about 18.60 m, and the minimum is only about 5.60 m.

Regarding the dynamic changes of sand dune landforms, as early as 1959–1964, the newly established Minqin Comprehensive Experimental Station of Desertification Control (MCESDC) in China carried out the field positioning observation and research on wind-blown sand flows in the Hexi Corridor (Zhu et al., 1980; Zhu and Chen, 1994; Zhu, 1999; Zhu and Wang, 1992; Wang, 2003). 187 positioning observation points were set up in field along a 20 km long observation line

in the Minqin Basin and many observations were made to assess the structure of wind-blown sand flow, the shape of sand dunes, erosion and accumulation of aeolian sand, changes in sand ripples and sand dune movement, etc. Later works continued to carry out relevant researches on different areas of the Hexi Corridor (Minqin Desert Control Experiment Station (MDCES), 1975; Zhu et al., 1980; Wang, 2003; Zhang et al., 2004; Qu et al., 2005; N. Wang et al., 2013; X. Wang et al., 2013; Yin et al., 2014; Yin et al., 2016; Chang et al., 2016, Chang et al., 2017; Zhang et al., 2016; An et al., 2019; Chang, 2019; Hu et al., 2020). In this study, we synthesized and collated these observational data and analytical results. It shows that in the Hexi Corridor, 80% of the sand particles of the wind-blown sand flows are moving in the height of 20–30 cm near the ground surface, of which about half of the sand particles are moving in the height of 0.3–0.5 cm near the surface. At the wind speed of 7 m/s, 75% of the sand particles are within the height of 10 cm, and only 0.035% are within the height of 76–200 cm.
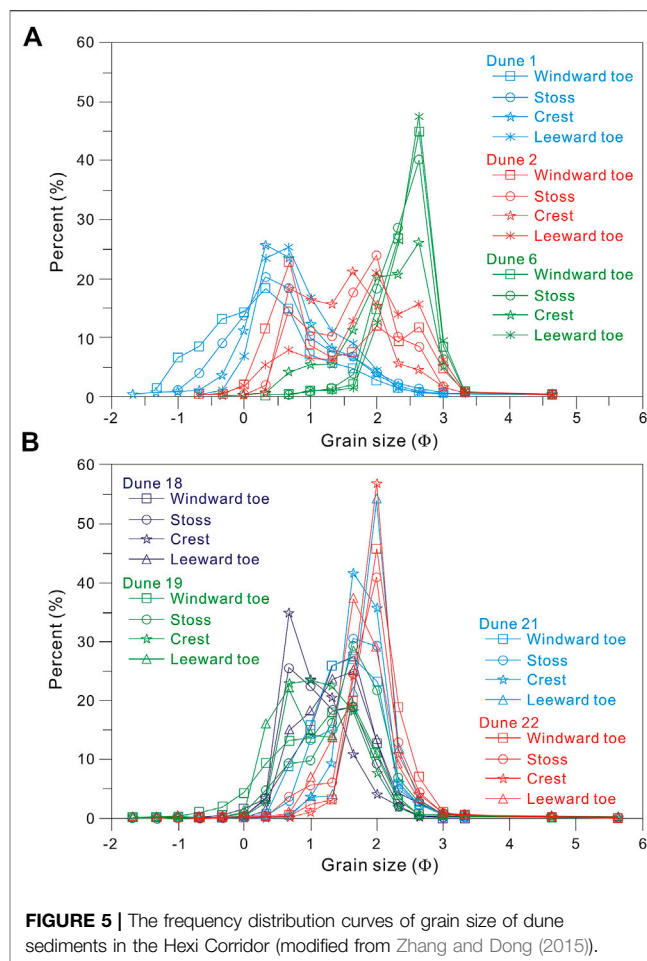
About the dynamic changes of different sand dunes in the Hexi Corridor in the past half century, the crescent-shaped (barchan) dunes, chains of barchan dunes, pyramid-shaped dunes, parabolic dunes, and longitudinal dunes have received

FIGURE 4 | The coefficient of variation (CV) plotted against the median grain size of classified surface sediment types in the Hexi Corridor (modified after Nottebaum et al., 2014). The coefficient of variation (CV) is an indicator of the degree of sorting process reflected by the standard deviation (StD), a discrimination parameter of GSD of sediment types. AS, aeolian sand; FS, fluvial sand; SWS, stillwater silt; SIL, silty loess; RSIL, reworked silty loess; SAL, sandy loess; RSAL, reworked sandy loess; SD, slope deposit.

the most extensive attention (e.g., Ren et al., 2010; Chang et al., 2016). Based on field surveys/measurements (e.g., measurement of the electronic total station) and digital image data (e.g., Google Earth) of different periods, the geomorphological parameters and moving speeds of these different dunes are obtained, as shown in **Tables 1–3** and **Figure 3**. It can be seen that the average moving speed of the crescent-shaped dunes is about 6.62 m/a in the study area, the maximum is 12.51 m/a, and the minimum is only 1.01 m/a (**Figure 3A**). The average moving speed of the chains of barchan dunes is about 6.54 m/a, the maximum is 8.30 m/a, and the minimum is only 5.34 m/a (**Figure 3B**). Compared with the crescent-shaped dunes, the chains of barchan dunes move relatively slowly and the movement speed changes little. In general, the crescent-shaped dunes and the chains of barchan dunes in the Hexi Corridor move along the NW-SE direction. The direction of movement of the east part of the corridor is about N45°W, while the movement angle of the Jinta area in the western corridor increases (**Table 1** and **Figure 3**). The average swing velocity at the tops of the pyramid dunes is about 6.32 m/a, the maximum is 97.37 m/a, and the minimum is only 1.14 m/a. The direction of movement of the pyramid dunes will also change, but its main direction of motion is SW-NE (**Figure 3**).

Surface Sediment Types and Granular Sedimentology of Sand Dunes in the Hexi Corridor

Analysis of grain size statistical parameters, geomorphological settings, sedimentological structures, and features to surface detrital sediments collected from different areas between the Qilian Mountains and their arid forelands (the Hexi Corridor) (e.g., Wang et al., 2008b; Wang et al., 2010; Wang, 2011; Nottebaum et al., 2014; Zhu et al., 2014; Zhu and Yu, 2014; Zhang and Dong, 2015; Pan et al., 2019) were performed. Parts of

FIGURE 5 | The frequency distribution curves of grain size of dune sediments in the Hexi Corridor (modified from Zhang and Dong (2015)).

these analytical results are comprehensively compared and re-analyzed by us and are shown in **Figures 4**, **5**. In general, six main sediment types can be classified in the Hexi Corridor based on the wide investigations of surface sediment distribution. They are fluvial sand, aeolian sand, sandy loess, silty loess, stillwater silts, and slope deposits (**Figure 4**). The term "stillwater silts" is firstly used by Nottebaum et al. (2014) to comprise altogether lacustrine, alluvial and mainly silty deposits in river channels (among which the latter are therefore neither lacustrine nor alluvial). A tripartite distribution of sedimentological landscape units in the Heix Corridor is evident, namely, the high mountain periglacial zone (from ~5,700 to ~3,800 m a.s.l.), the loess altitudinal zone (from ~3,800 to ~2,000 m a.s.l.), and the foreland zone (<2,000 m a.s.l.) (Nottebaum et al., 2014). Dune fields are limited to areas below 1700 m a.s.l.

At a regional scale of the study area and compared to other types of surface detrital sediments in the Hexi Corridor, the movement modes of aeolian sand particles in the study area include creeping (wriggling/rolling), saltation (jumping/springing) and suspension (floating/levitating), and the movement modes of sand dunes include three ways: straight-forward movement, wigwagging movement, and onward-wigwagging movement (Wang, 2003; Zhu et al., 2014). Aeolian sands collected from dune ridges and sand sheets in

surface sediment investigations in the study area are usually best sorted (Nottebaum et al., 2014; Zhu and Yu, 2014). It can be evidenced by low CV values of 24–85 for aeolian sands in the study area and mostly have unimodal grain size distributions (GSDs) (**Figures 4**, **5**). Among this sediment type (aeolian sand), bimodal distributions (**Figure 5**) may be mixtures of loess and aeolian sand or due to mixing of two aeolian sand populations (Nottebaum et al., 2014; Zhu et al., 2014). The general modal values of aeolian sands' GSD typically cluster around ~200 μm in the study area. In contrast, aeolian samples with finer modes occur at small vegetated dunes where wind speeds are reduced due to locally higher surface roughness, and aeolian samples with larger mode values originate, for example, from barchans (mode = 430 μm) or coarse sand ripples (mode = 825 μm) (Nottebaum et al., 2014). This type is mainly formed by saltation and creeping processes, accumulating grain sizes determined by wind speed and source material properties (Zhu et al., 2014). These dunes and sand sheets are restricted to the lowland areas, overlying the foreland alluvial fans, and are interchanging with oases and agricultural areas.

At the local scale, dune sands in different regions also have different sedimentological characteristics, especially between the middle-East and the west of the study area. Basically, the eastern parts of the Hexi Corridor show higher aeolian sand occurrence. In contrast, the western parts are dominated by gravel gobi surfaces. This is possibly attributed to higher sand supply in eastern parts provided by the Badanjilin Desert and fluvial storages as sand sources (Nottebaum et al., 2014).

In the Jiuquan-Gaotai area in the central-eastern Hexi Corridor (area B in **Figure 2**), grain size parameters of sand dunes at different geomorphological positions on the dune surface were determined (**Figure 5**), such as the toes of windward slope, slope surface, dune crest (top), toes of leeward slope, etc. The results show that the grain-size frequency distribution curves of sand dunes in this area are mostly unimodal, and a few are bimodal (**Figure 5**). The dune surface sands are mostly fine sand and very fine sand, with an average grain size of 0.07 mm ± 0.01–0.24 mm ± 0.06, which is similar to the average particle size of sand dunes in the world (Zhu et al., 2014; Zhang and Dong, 2015). The finer the dune particle is, the better the sorting degree is. The mean grain size increases with the increase of the skewness values, but decreases with the increase of the kurtosis values. From upwind to downwind, the dune sediment becomes finer, the medium-sand fraction decreases, and the fine-sand fraction, very-fine-sand fraction, silt-fraction, and clay-fraction increase. It may be the source materials that affect the changes in the average grain size of dune sands from upwind to downwind (Zhang and Dong, 2015). In this dune field, there are three types of grain-size-distribution patterns in a dune-scale unit: the dune crest is coarser (the dune slope and inter-dune area are finer), the dune crest is finer (the dune slope and inter-dune land are coarser), and there is no significant difference between dune crest, windward and leeward slopes. Among them, the coarser-dune-crest model is the most common type, accounting for 69% of all sand dunes, while the finer-dune-crest is the second most common type (accounting for 24%) (Zhang and Dong, 2015).
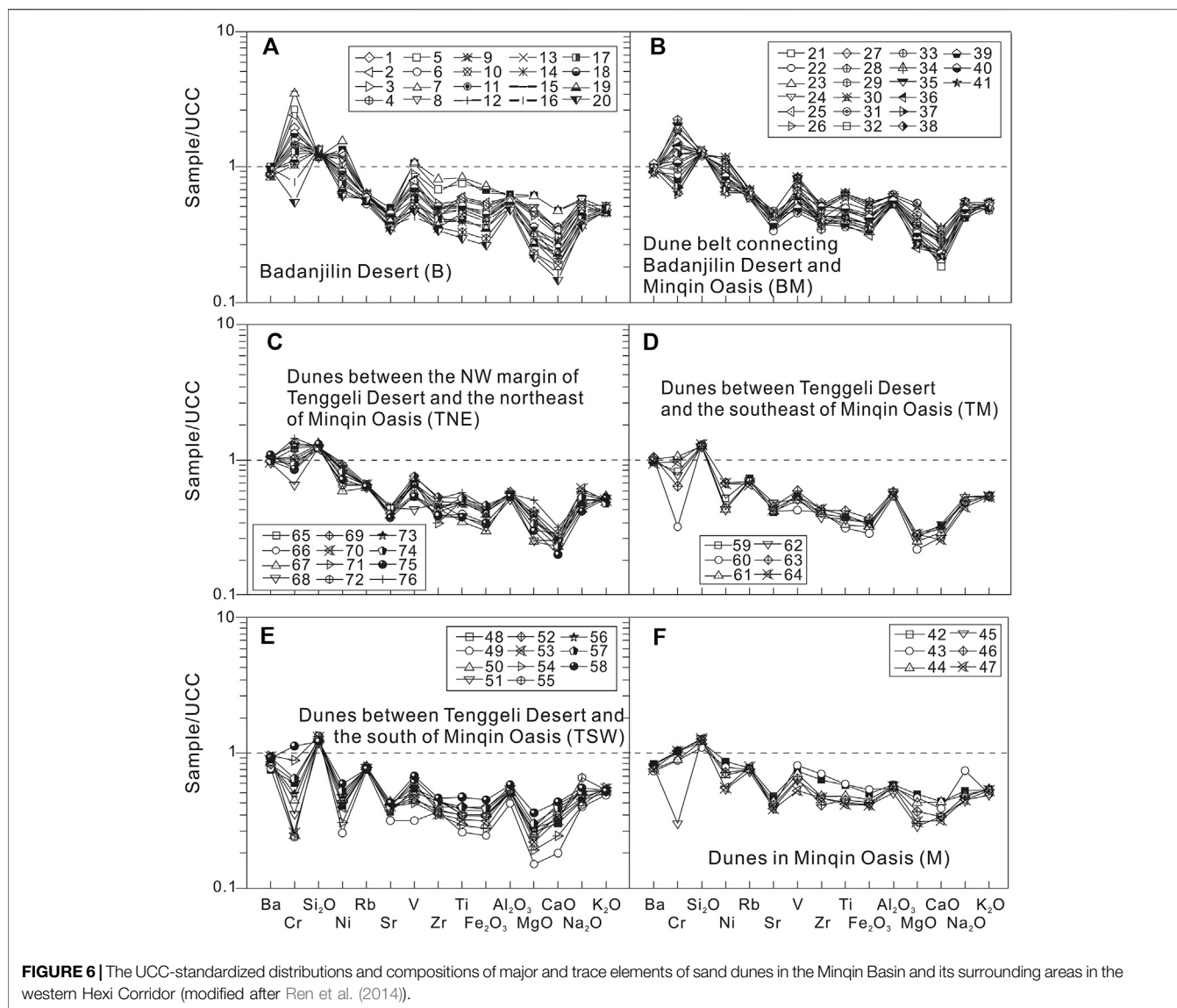
In the Jinta-Jiayuguan-Huahai area in the western Hexi Corridor (area A in **Figure 2**), granular sedimentology of the crescent-shaped (barchan) dunes developed on gobi deserts and ancient playas have been determined (e.g., Pan et al., 2019). The results show that the grain size of dune surface sediments is mainly the medium sand (21.7–57.4%), followed by the fine sand (23.2–53.0%). The mean grain size of dune sands range between 0.27 and 0.43 mm, while the paleolacustrine sediments range between 0.10 and 0.21 mm. The crescent-shaped dune sediments in this region are mainly medium to good in the sorting level. The frequency cumulative curves of dunes are mostly unimodal and nearly symmetrical, and the kurtosis is medium in level. The granular characteristics of sand dunes in this region are closely linked to their dune morphology and the properties of the underlying gobi surface (Pan et al., 2019).

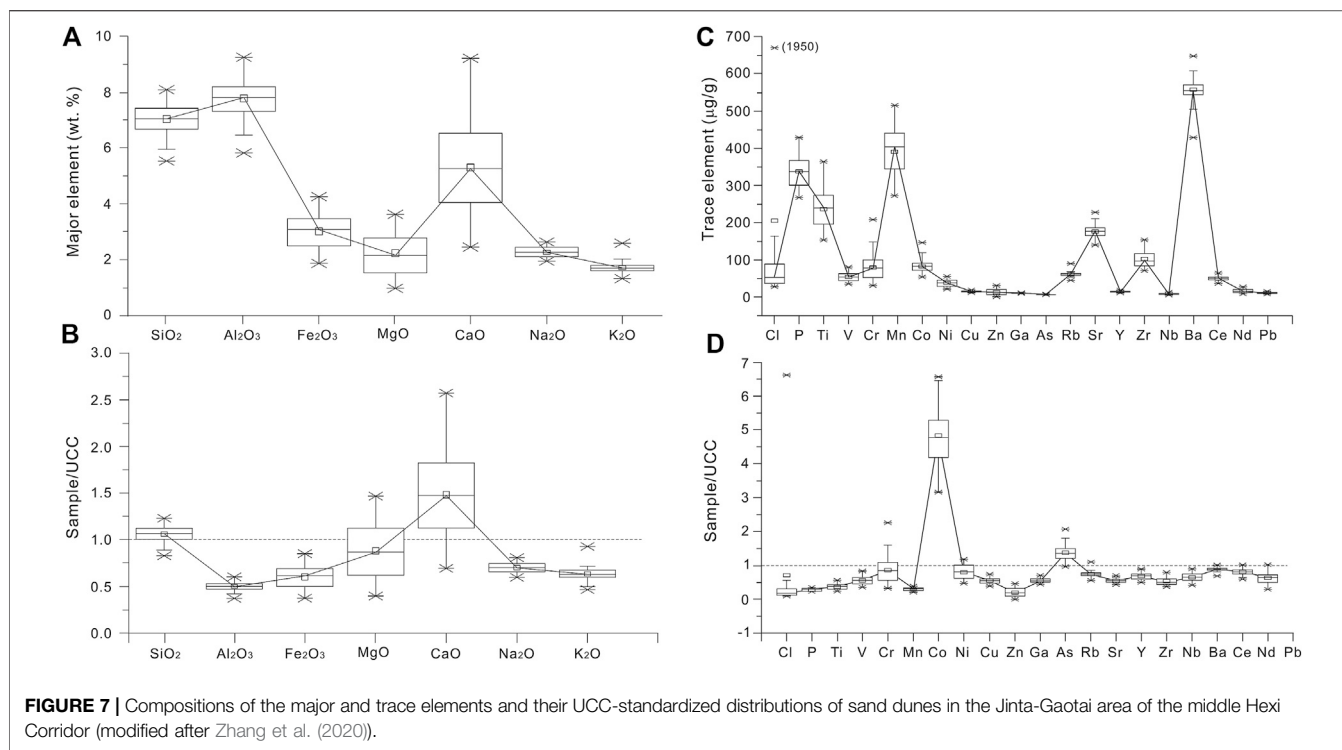## Geochemical Characteristics of Dune Sediments and Soil Aggregate in the Hexi Corridor

Due to the application of geochemical methods in recent years, it is possible to identify sediment sources more precisely. The geochemical characteristics of aeolian sediments in the Hexi Corridor had been investigated as early as 1959–1964 by the China's Minqin Comprehensive Experimental Station of Desertification Control (MCESDC) (Minqin Desert Control Experiment Station (MDCES), 1975; Zhu et al., 1980; Chang, 2019), and continues to this day (Wang et al., 2010, Wang et al., 2018; Ferrat et al., 2011; Wang, 2011; Ren and Wang, 2010; Wang and Wang, 2013; Ren et al., 2014; Zhang and Dong, 2015; Zhang et al., 2016, Zhang et al., 2020; Chang, 2019; Pan et al., 2019). In this study, based on the integrated geochemical data, we explored the material sources of dune sands in the study area at different regional scales, as shown in **Figures 6**, **7**. We take the Minqin Basin in the eastern Hexi Corridor (area C in **Figure 2**), the Huahai-Jiayuguan-Jinta region of the western Hexi Corridor (area A in **Figure 2**), and the Jinta-Gaotai region of the middle Hexi Corridor (area B in **Figure 2**) as the case examples to discuss in detail.

The Minqin Basin in the eastern Hexi Corridor (area C in **Figure 2**) is dominated by an oasis landscape. It is bordered by the Badanjilin Desert to the northwest and the Tenggeli Desert to the southeast and is located the northern edge of the Loess Plateau (**Figures 1**, **2**). In geomorphology the Minqin Basin is considered a natural obstacle to the convergence of the two deserts (Zhu et al., 1980), thus identifying the origin and transportation of aeolian sediments in the Minqin oasis and its adjacent desert areas will help to better understand the relationship between loess and desert in China (Liu, 1985; Sun, 2002; Yang et al., 2007; Wang et al., 2010; Yang et al., 2011; Ren et al., 2014). Aeolian sediments sampled from sand dunes in the Minqin Oasis and its surrounding desert areas (the Badanjilin and Tenggeli Deserts) have been geochemically studied recently (e.g., Ren, 2010; Ren and Wang, 2010; Ren et al., 2014). In this study, the characteristics of major and trace elements of aeolian samples from the Minqin Oasis and its adjacent deserts, as well as the provenance and transportation pathways of aeolian sediments in these areas, were discussed using these integrated geochemical data, combined with wind data and cluster analysis methods, as shown in **Figure 6**.

FIGURE 6 | The UCC-standardized distributions and compositions of major and trace elements of sand dunes in the Minqin Basin and its surrounding areas in the western Hexi Corridor (modified after Ren et al. (2014)).

The analytical result shows that in the bulk (whole-rock) samples of dune sands in the Minqin Basin (M) and its surrounding areas, including the Badanjilin Desert (area B), the Badanjilin-Minqin transition zone (area BM), the Tenggeli-Minqin transition zone (area TM), the northeast edge of the Tenggeli Desert (area TNE), and the southwest edge of the Tenggeli Desert (area TSW) in **Figure 6**, the contents of major elements are higher in SiO_2, reaching between 72.2 and 88.9% with an average of about 83.3%. In contrast, the contents of most trace elements are relatively low, and only the contents of Ba, Ce, Co, Mn, and Sr reach > 100 ppm. Compared with the average composition of the upper continental crust (UCC, Taylor and McLennan, 1985), the concentrations of Ba, SiO_2, Rb, Sr, Al_2O_3 and K_2O in the Minqin Basin and its surrounding areas are relatively uniform (**Figure 6**), indicating that the spatial differences of these elements in abundance are small and they are relatively homogeneous in the study area. However, obvious convex and concave shapes are observed for other elements

(**Figure 6**), indicating that the spatial differences of these elements in abundances are large and they are relatively heterogeneous in the study area. The homogeneous and heterogeneous characteristics between different elements thus can be used as geochemical indicators to identify different sources of sediments in the study area. For the major elements' compositions, only SiO_2 is enriched relative to UCC, and the others are relatively depleted (**Figure 6**). For the trace elements' abundance, most elements are also depleted, except for Cr and Ni enriched in areas B and BM and Cr enriched in area TNE. The binary and ternary diagrams of some major and trace elements and their ratios (Ren et al., 2014), such as Cr, Ni, Cr/V, Y/Ni, Al, V, Zr, Hf, Zr/Hf, reveal that sand dunes have different material sources between the western part of the Minqin Basin (including sub-areas B, BM and TNE) and the southeast side of the Minqin Basin (TSW), while sand dunes in the Minqin Basin (M) and the Tenggeli-Minqin transition zone (TM) are closely related to the two big deserts, respectively.

FIGURE 7 | Compositions of the major and trace elements and their UCC-standardized distributions of sand dunes in the Jinta-Gaotai area of the middle Hexi Corridor (modified after Zhang et al. (2020)).

In the western Hexi Corridor, data of major and trace elements of aeolian sediments and other types of sediments sampled in this region are also synthesized and integrated in this study based on previous studies (e.g., Wang et al., 2010; Zhang et al., 2017; Pan et al., 2019). The sand dunes analyzed in this study are mainly located in the gobi areas to the northern and western Jiayuguan (area A in **Figure 2**). The dune types are mainly barchan dunes, chains of barchan dune and asymmetric barchans dunes (Zhang et al., 2017; Pan et al., 2019). The aeolian samples were mainly collected from the surface sediments of barchan dunes and asymmetric barchan dunes, including different geomorphic sites of dunes such as the crest of dune, the bottom of the windward slope, the middle of the windward slope, and the bottom of the leeward slope. The analytical results show that after the standardization of UCC, the barchan dunes on the Gobi surface in the western Hexi Corridor are significantly enriched in the major elements CaO and SiO_2 (accounting for 5.55 and 66.12% of the total rock mass, respectively). In terms of spatial distribution, the element contents of Cao, MgO and Fe_2O_3 are gradually enriched from northwest to Southeast, that is, the enrichment degree increases along the dominant wind direction. The UCC-normalized concentrations of Na_2O and K_2O are both significantly <1, indicating that alkali metal elements are significantly depleted or leached in the study area. The contents of trace elements vary among different dune samples, reflecting a complexity of provenance of these dune sediments. However, the variations of trace elements are similar in different geomorphic positions of the one dune (Pan et al., 2019). Compared with UCC, trace elements Co, As, La, and Nd are significantly enriched in the western Hexi Corridor, while other elements are depleted.

In the middle Hexi Corridor, mineralogical, major- and trace-element data of aeolian sediments and other types of sediments from the Jinta-Gaotai area (area B in **Figure 2**) are also collected and integrated in this study based on previous studies (e.g., Ferrat et al., 2011; Wang and Wang, 2013; Wang et al., 2018; Zhang et al., 2020). Indicators such as the light/heavy mineral assemblages, the ratios of Na_2O/Al_2O_3 to K_2O/Al_2O_3 and SiO_2/Al_2O_3, Ba/Sr to Rb/Sr, Rb/Sr to Ce/Sr, and the composition of CaO and Cl in the sampled aeolian sediments are used to identify the geochemical characteristics of aeolian sediments in the study area, as shown in **Figure 7**. Compared with the composition of the upper continental crust (UCC), dune sediments in the Jinta-Gaotai area are also enriched in CaO and SiO_2 (**Figure 7**). Based on analysis of multi-dimensional scaling (MDS), principal component analysis (PCA) and regional topography analysis (e.g., Zhang et al., 2020), the results suggest that the Hexi Corridor is not only the sediment sink of the Qilian Mountains, but also the sediment sink of the Beishan Mountains.

Compared with the chemical elements in the Tenggeli and Badanjilin Deserts (Li, 2011), the Hexi Corridor has lower SiO_2 content, similar K_2O content, and lower contents of other trace elements. However, in terms of major- and trace-element ratios, the sand dunes from the Hexi Corridor are similar in provenance to those from the Tenggelil, Badanjilin, and Kumtag Deserts (Zhang et al., 2020). Similar mineralogical assemblages (mica, quartz, illite, muscovite and albite) are also found in dune sediments from the Hexi Corridor and adjacent areas such as the Tenggeli and Badanjilin Deserts (Ferrat et al., 2011). This feature is also found by major and trace element analysis in other studies (Wang and Wang, 2013; Zhang et al., 2020). This

indicates that the geochemical characteristics and provenance of aeolian sediments in the Hexi Corridor are closely related to its adjacent areas.

Soil aggregate, as the basic unit of farmland soil structure, is widely developed in oasis areas of the Hexi Corridor (Li, 2006; Su, 2007). It plays important role in surface nutrient recycling, resisting soil wind and water erosion, and are closely related to dust emission and land desertification in arid land (Bronick and Lal, 2005). Thus, the mechanisms of formation and stability of soil aggregate are one of the major topics in land degradation/development science in arid environment (Le, 1996; Bronick and Lal, 2005). In order to determine the geochemical characteristics of soil aggregates, soil samples at the 0–10 cm surface layer from different soil types (i.e., Ari-Sandic Primosols, Calci-Orthic Aridosols, Siltigi-Otrthic Anthrosols, and Ustic Cambosols, etc.) in the marginal farmland in the oasis of the middle Hexi Corridor have been studied (e.g., Li, 2000, Li, 2006; Su, 2007; Su et al., 2007). In this study, we briefly review the results of previous studies.

The physiochemical properties of dry- and wet-sieved soil aggregates in the middle Hexi Corridor, including soil particle-size distribution (SPD), soil organic carbon (SOC), calcium carbonate ($CaCO_3$), and oxides of Fe^{3+} and Al^{3+}, were analyzed (e.g., Li, 2000, Li, 2006; Su, 2007; Su et al., 2007). The results show that the SPD is dominated by fine sand fraction in most of soils except Ustic Cambosols. The SOC concentration is 5.88 ± 2.52 g/kg on average, ranging from 4.75 g kg^{-1} in Ari-Sandic Primosols to 10.51 g kg^{-1} in Ustic Cambosols. The soils have high $CaCO_3$ concentration, ranging from 84.7 to 164.8 g/kg, which is increased with fine SPD and SOC content. The percentage of >0.25 mm dry aggregates ranges from 65.2% in Ari-Sandic Primosols to 94.6% in Ustic Cambosols, and large dry blocky aggregates (>5 mm) is dominant in all soils. The mean weight diameter of dry aggregates (DMWD) ranges from 3.2 to 5.5 mm. The percentage of >0.25 mm water-table aggregate is from 23.8 to 45.4%. The percentage of aggregate destruction (PAD) is from 52.4 to 66.8%, which shows a weak aggregate stability. The mass of macro-aggregates and DMWD are positively significantly correlated with the contents of soil clay and silt, SOC, $CaCO_3$, and oxides of Fe^{3+} and Al^{3+}. Soil fine silt and clay, SOC and $CaCO_3$, are important agents of aggregation in this region, and the effect of SOC and $CaCO_3$, on aggregate stability is more significant than that of soil silt and clay.

DISCUSSION

Dynamic Changes of Dune Landforms in the Hexi Corridor

The above analytical results of geomorphological parameters indicate that the dynamic changes of different dunes are different in the Hexi Corridor during the past several decades. Among different dune types, the crescent-shaped dunes move the fastest, followed by the chains of barchan dunes (**Figure 3**). Only the top of the pyramid dunes wigwags (**Figure 3**), while the parabolic dunes and the longitudinal dunes hardly move forward (Chang et al., 2016). We seem to be able to come to this view that the higher the height of the crescent-shaped dune (or the chain of barchan dunes) is, the slower their movement is. On the contrary, the higher the height of the pyramid dunes is, the faster they swing. The above analysis also suggests that the moving speed of sand dunes in the study area is positively correlated with the local wind speed ≥5 m/s of local climate at a yearly scale.

Here, we compare the moving speed of sand dunes in the Hexi Corridor with that in other sandy desert areas in northwestern China. In the Taklamakan Desert, the largest sand desert in China, the observation results of eight crescent-shaped dunes along the oil transportation highway showed that the moving speed of sand dunes was 4.81–10.87 m in October 1991–1992, with an average of 7.29 m, and the moving speed of these sand dunes was 3.33–8.89 m in October 1992–1993, with an average of 5.56 m (Dong et al., 1998). Based on the digital interpretation results of high-resolution remote sensing images during the period 2010–2014, the average speed of dune movement in the Tenggeli Desert was 4.36 m/a in 2010–2013, and was 2.43 m/a in 2013–2014 (Hu et al., 2016). Based on the digital interpretation results of high-resolution Google Earth QuickBird images during the period 2002–2010, the moving speeds of 22 crescent-shaped dunes in the Maowusu Sandy Land are between 3.5 and 9.5 m/a (J. Wang et al., 2013). The width of these dunes is significantly correlated with the horizontal length of the leeward slope of the dunes, and the width of the dunes and the horizontal length of the leeward slopes decrease during the movement of dunes, while the horizontal length of the windward slopes increases. There is a good correlation between the moving speed and the width of dune.

It can be seen from the above that the moving speeds of sand dunes in different desert areas are quite different. Compared with sand dunes in the deserts mentioned above, the moving speed of the widely distributed crescent-shaped dunes in the Hexi Corridor also varies greatly. During the period 2006–2015, sand dunes at the edge of the Minqin Oasis area moved the fastest, with a moving speed of about 6.2 m/a, while sand dunes at the edge of the Dunhuang Oasis moved the slowest, with a moving speed of only about 0.8 m/a (**Figure 3**). The horizontal length of the windward slope of sand dunes in most areas of the Hexi Corridor increased in 2015 compared with that in 2016, while the horizontal length of the leeward slope of sand dunes decreased (**Tables 1**, **2**).

Summarizing the above characteristics of geomorphological parameters of different dunes, it can be concluded that there are two states of sand dunes movement in the Hexi Corridor in the past half century, dynamic migration and basically stable. This kind of geomorphological evolution of dunes is possibly closely related to their material sources and regional environmental conditions.

Depositional Environmental and Transportation Modes of Sand Dunes in the Hexi Corridor

The above analytical results of grain size of aeolian sediments from the Hexi Corridor have shown that sand dunes have different grain size compositions in different regions of the Hexi Corridor (**Figures 4**, **5**). It is obvious that the average

grain size of sand dunes in the western Hexi Corridor (such as the Huahai-Jinta-Jiaquan area, average 0.27–0.43 mm) is larger than that in the central-eastern Hexi Corridor (such as the Jiuquan-Gaotai-Minqin area, average 0.07–0.24 mm) and also larger than those in other desert regions of northern China (average 0.17–0.19 mm, Zhu et al., 2014; Zhu and Yu, 2014) and of the world (average 0.11–0.23 mm, Lancaster, 1995).

The spatial differences in grain size compositions may reflect the different depositional environment, the different sources and the different transportation modes in the formation and development of sand dunes in the Hexi Corridor. According to the grain-size discriminant function proposed by Sahu (1964), the major sedimentary environment in the Hexi Corridor includes three types of deposits, i.e., aeolian deposit, lacustrine deposit and alluvial-proluvial deposit (**Figure 4**), of which aeolian deposit is the dominant (about 50%) (Nottebaum et al., 2014; Zhang and Dong, 2015). Compared with the crescent-shaped dunes in the central-eastern Hexi Corridor, the shrub dunes in the western Hexi Corridor are dominated by the medium- to fine-sand fractions, but not the medium-sand fraction. This is possibly because of the wide distribution of gravel around the shrub dune, which reduce the airflow velocity near the ground, making it difficult for the coarser-grained particles to move up to the surface of shrub dunes (Zhu et al., 2014). While for the crescent-shaped dunes, the length of wind flow path on the windward side of the dune is longer. During the movement of the unsaturated aeolian sand flow, the coarser-grained particles collide with the ground surface elastically, resulting in the coarser-grained particles moving to a higher position on the windward slope of crescent-shaped dune, so the crescent-shaped dunes are dominated by the medium-sand-fraction particles. The clay-grain content is less in the surface layer of the crescent-shaped dunes and the shrub dunes, but more (up to 28.2%) in sand dunes developed on dry lake beds (playas) or ancient lake area, which is obviously related to the local source of fine particles.

Generally, the probability cumulative curve of grain size of aeolian sediments in the world is usually shown as two to four independent line segments, indicating that two to four modes of motion occur during their transportation (Visher, 1969). The probability cumulative curve of grain size of sand dunes in the Hexi Corridor basically presents a three-stage pattern truncated at about 1.8φ (coarse group) or 2.5φ (fine group) (**Figure 5**), indicating that sand dunes in the study area are dominated by the motion mode of saltation under the action of wind, and superimposed with a small number of particles transported by the motion modes of suspension and creeping. This feature has been observed in sand dunes in different areas of the Hexi Corridor including the lower reaches of the Heihe River Basin near the Hexi Corridor (Zhu et al., 2014; Zhang and Dong, 2015; Zhang et al., 2016; Pan et al., 2019). But compared with dune sediments, the movement modes of gobi sediments and lacustrine sediments in the Hexi Corridor are mainly creeping-saltation and saltation-suspension, respectively (Zhu and Yu, 2014; Zhang et al., 2016), indicating different motion modes between aeolian, lacustrine and gobi sediments. The differences can also be

reflected from the frequency distribution curves of these sediments, as dune sediments are usually unimodal distribution (**Figure 5**), while aqueous and gobi sediments are bimodal or multimodal distribution (Zhu, 2007; Zhu and Yu, 2014).

Sources of Sand Dunes in the Hexi Corridor

The above geochemical analysis provides good evidences for the understanding of the material sources of sand dunes in the Hexi Corridor. The result that sand dunes in the Minqin area have different material sources between the western part (the Badanjilin-Minqin transition zone), the central part, the southeast side, and the eastern part (the Tenggeli-Minqin transition zone) of the Minqin Basin indicate that aeolian sediments from the Badanjilin Desert can be transported to the west side of the Minqin Oasis through mountains (Yabulai) for a long distance by the northwest wind, and aeolian sediments from the Tenggeli Desert provide material source to the east side of the Minqin Oasis. However, the aeolian sands of the two sandy deserts cannot reach or bypass the other side of the oasis to achieve a confluence of the two deserts. This reveals that the Minqin Oasis is real an effective barrier to prevent the migration and convergence of sand dunes between the Badanjilin and Tenggeli Deserts. However, the large number of aeolian dunes developed in and around the Minqin Basin also suggests that the role of oasis in preventing eaolian erosion is limited and should not be overestimated.

Comparing the major element abundances of aeolian sediments in different deserts of China (**Table 4**), the sand dunes in the Hexi Corridor have certain differences and similarities with deserts in northern China. For example, the content of Fe_2O_3 in sand dunes of the Hexi Corridor can reach 3.50%, which is generally higher than any one of other deserts in China, while the contents of other elements in the Hexi Corridor are in a similar range of element abundance to those of other deserts, indicating that the sand dunes in the Hexi Corridor are rich in iron element. Compared with the composition of the upper continental crust (UCC), dune sediments in the middle and eastern Hexi Corridor are enriched in SiO_2 (**Figures 6**, **7**) and CaO (**Figure 6**), which are similar to those in the fluvial and lacustrine sediments near the Taklamakan and Badanjilin Deserts and the aeolian sediments in the surrounding gobi desert, but they are slightly different from those in the Kumtag and Tenggeli Deserts (Zhang et al., 2020).

The analytical results from heavy mineral assemblages and trace element abundances indicate that the provenance of sand dunes in the Hexi Corridor is mainly from "sands of *in-situ* rising," which is also the genetic mechanism of many desert sands in northern China (Zhu et al., 1980; Yang, 2006; Yang et al., 2007, Yang et al., 2012; Chang, 2019). In this study, the structural distribution of wind-drifting sand flow in the Hexi Corridor and its relationship with wind speed also support this point. The above results show that most part of sand particles in the Hexi Corridor are transported near the ground surface (0.3–10 cm) when the wind speed is < 7 m/s. This implies that if there are any small topographical fluctuations (>20 cm) on the surface of the

TABLE 4 | The average element contents (%) of sand dunes in the Hexi Corridor and other deserts and the average composition of the upper continental crust (UCC). CLP, the Loess Plateau in China.

Regions	Fe_2O_3	CaO	MgO	SiO_2	Al_2O_3	Na_2O	K_2O	References
Hexi Corridor	3.5	5.55	2.07	66.12	9.24	2.45	2	Zhang et al. (2017), Pan et al. (2019)
Badanjilin Desert	1.93	2.06	1.19	80.27	7.78	1.9	2	Zhu and Yang, (2009)
Tenggeli Desert	1.96	1.3	1.12	80.94	8026	1.88	2.25	Zhu and Yang, (2009)
Kumutage Desert	2.88	4.64	2.19	70.13	9.59	2.52	1.98	Dong et al. (2011)
Taklamakan Desert	3.1	7.88	2.2	62.05	10.6	2.58	2.11	Zhu and Yang, (2009)
Loess (CLP)	4.56	8.62	2.31	58.65	11.86	1.68	2.44	Dong et al. (2011)
paleosol (CLP)	5.12	0.83	2.21	65.18	14.79	1.41	3.15	Dong et al. (2011)
UCC	5	4.2	2.22	66	15.2	3.9	3.4	Taylor and McLennan, (1985)
Terrestrial shale	7.22	1.3	1.2	62.8	18.9	1.2	3.7	Taylor and McLennan, (1985)

TABLE 5 | Meteorological data of sandstorm and strong wind in the Hexi Corridor (cited from Chang et al. (2015)).

Weahter station	Average wind speed (m/s)	Wind speed ≥ 8 grade/d	Sandstorm days (d)	Maximum wind direction
Gulang	3.5	4.5	4	NW
Wuwei	1.8	9.7	4.8	NW
Minqin	2.7	25.1	27.4	NW
Jinchang	3.3	25.1	27.4	NW
Yongchang	3	24.6	4.2	NW
Zhangye	2	12.2	11.8	NW, SSE
Linze	2.5	21.7	7.7	NW
Gaotai	2	7.8	11.1	NW
Jiuquan	2.2	16.6	10.3	NNW
Jinta	1.9	14.4	6.4	NW, WNW
Yunmen	3.8	40.6	8.1	WNW
Average	2.61	18.39	11.2	—

study area, it is difficult to transport and migrate these aeolian sands for a long distance to be far away from their source areas. Palaeogeographical and geomorphological studies (e.g., Minqin Desert Control Experiment Station (MDCES), 1975; Zhu et al., 1980) believe that sediments from alluvial plains and alluvial deposits of ancient rivers, lacustrine plain and lacustrine deposits of ancient lakes, aeolian deposits in the erosion zone of the forelands of the northern Qilian Mountains and the southern Beishan Mountains, and alluvial and fluvial deposits of modern rivers are the main material sources of sand dunes in the Hexi Corridor. Based on mineralogical analysis, Ferrat et al. (2011) observed that sand dunes in the Hexi corridor have similar concentrations of mica, quartz, illite, muscovite and albite with adjacent areas, such as the Tenggeli Desert and the Badanjilin Desert. This similar mineralogical composition may lead to the similarity in geochemical characteristics of aeolian sediments in these areas. Geochemical and grain-size analysis of detrital sediments collected from alluvial deposits in the Qilian Mountains, paleo-lacustrine deposits in low-level areas, and surface aeolian sediments in gobi desert areas of the southern Beishan Mountains (e.g., Wang and Wang, 2013; Zhang and Dong, 2015; Zhang et al., 2016; Zhang et al., 2020), also suggest that these regions are the main source areas of sand dunes in the Hexi Corridor.

In addition to the above comparisons from geochemical evidences of aeolian sediments at a regional scale, the local landform type and spatial distribution characteristics and their relationship with the dominant wind/river conditions also provide clues to explore the potential source of sand dunes in the Hexi Corridor.

Most active dune fields in the Hexi Corridor are located between the cities of Jinta and Zhangye and at the margin of Badanjilin Desert (**Figure 2**). The desert marginal dune fields can be regarded to be directly linked to the sand deserts (e.g., Badanjilin and Tenggeli). The above geochemical evidences also support this point. From the local dominant wind conditions in different areas of the Hexi Corridor (**Table 5**), these dunes are subjected to strong northerly winds. This suggests sand transport from the desert into the southerly bordering Hexi Corridor. A southward transport can also be indicated by the linear dune field in this region (Nottebaum et al., 2014). Monthly averaged wind directions for Zhangye show a bimodal pattern (dominant wind directions from northwest and south-southeast, **Table 5**) from May to July, which is the transition period of winter monsoon to summer monsoon dominance (Bourque and Mir, 2012). Nevertheless, as wind speeds are higher in spring (Ta et al., 2004) a positive balance of southward sand transport is likely. Therefore, the Badanjilin Desert is probably the dominant source region for the northern dune fields in the Hexi Corridor. In contrast, dune fields between Jinta and Zhangye are located south of the braided Heihe River valley and in vicinity to the Qilian Mountains front (**Figure 2**). As the Heihe River forms a barrier for saltating sand

grains moving south from the Badanjilin Desert, the source regions for the southern dune fields in the Hexi Corridor are suspected to be in the braided Hei River valley and the foreland alluvial fans. This is evident as they are directly connected to fluvial channels breaking through the Qilian Mountains front (Nottebaum et al., 2014).

Different transport of aeolian sand in the western Hexi Corridor is evidenced by isolated barchans dunes with coarser grain sizes than dune fields in the eastern part (**Figure 5**). Hence, a sufficient transport capacity is evidenced. However, dune fields are rare in the western part of the Hexi Corridor. This region is not close to sand deserts but bare low mountains, such as the Beishan Mountains to the north (**Figure 2**). Regarding to the distribution of clastic materials, the northerly bordering Beishan Mountain exhibits vast areas of bare primary weathering rock surfaces. However, according to Kocurek and Lancaster (1999), material for "terrigenous dune fields" is rarely a product of primary rock deflation, but rather results from fluvial deposits, therefore, it has only limited potential to serve as a productive source area for large amounts of sand compared to fluvial deposits (Kocurek and Lancaster, 1999). Additionally, fluvial sand supply from Qilian Mountains is limited as contributing rivers are ephemeral. These conditions are in clear contrast to those in the eastern part of the Hexi Corridor: in the latter, the Badanjilin Desert exposes large amounts of well-sorted aeolian sands to northerly winds, and additionally, perennial Heihe River and the mountain proximal alluvial fans can also serve as sand suppliers for the east part. Therefore, sufficient sand supply and sand availability is provided for the formation of sand dunes in the eastern part of the Hexi Corridor, but not for dunes in the west part. Generally speaking, sufficient transport capacity is evidenced for both the western and eastern parts of the Hexi Corridor, sufficient sand supply and sand availability, however, is the limiting factor for dune field formation in the west part of the Hexi Corridor.

Summarizing the above geochemical, geomorphological, and sedimentological characteristics and related environmental evidences of sand dunes, it can be concluded that dried river deposits (playas), alluvial/proluvial deposits, neighboring desert sands are the main sources of sand dunes in the Hexi Corridor. While the initial provenance of these aqueous and aeolian deposits mainly come from the forelands/foothills of the Qilian Mountains in the south and the Beishan Mountains in the north via river transportation. This reveals that the interaction between wind and water dynamics is of great significance in the formation and evolution of aeolian landforms in terms of geomorphic genesis in arid areas.

## Formation of Shrub Dunes in Oasis Area of the Hexi Corridor

Compared with sand dunes in desert area, many sand dunes inside the oasis area of the Hexi Corridor are shrub dunes and have more complex material sources. They are closely linked to regional land degradation and desertification issues in the Hexi Corridor.

In the arid and semi-arid areas of northern China, the occurrence of desertification or reverse desertification (restoration) is closely related to the interaction of local aeolian and fluvial processes (Wang et al., 2008b). Studies have shown that in the past 50 years, desertification and restoration in

northern China usually occurred in alluvial plains or flood plains caused by changing hydrological conditions, where the sandy sediments derived from floods and rivers are deflated and reworked by wind (Li et al., 2002). Moreover, the soils that are originated from these parent materials, such as aeolian sandy soil, brown soil, cinnamon soil, gray cinnamon soil, chernozem and karst soil, are also vulnerable to wind deflation and water erosion and thus easily degenerated and degraded (Yang, 1985; Liu et al., 1998; Wang et al., 2008b).

In the middle and eastern areas of the Hexi Corridor, the oasis and surrounding desert landscapes exit paradoxically to a certain extent, with a relationship of being independent and interdependent between them. Although sand dunes also exist inside the oasis, the surface clastic materials are mostly soil aggregates. The potential relationship between aeolian sand and soil aggregates is a basis for understanding the formation of sand dunes in the oasis area. The above analysis has shown that in the oasis areas of the middle Hexi Corridor, most surface soils are characterized by high sand content, low SOC level, and were rich in calcium carbonate. These soils are prone to disperse and harden after irrigation. The large blocky aggregate at the size of >5 mm is the dominant fraction in aggregate size distribution in surface soils, which is in favor of resisting soil erosion by wind. After wet sieving, most macro-aggregates broke down and dispersed, indicating a weak stability. The contents of clay, silt, SOC, $CaCO_3$, Fe_2O_3, and Al_2O_3 had significant influence on the formation of aggregates. The total percentage of dry aggregates and DMWD are more correlated with clay and silt content than SOC and $CaCO_3$ content, although the effect of SOC and $CaCO_3$ content on wet-sieving aggregates were more significant than that of clay and silt content. From the above results, it can be concluded that the distribution and characteristics of soil aggregates in oasis areas of the Hexi Corridor are in favor of controlling soil wind erosion. However, the stability of all soil aggregates is weak in the study area after irrigation. That is to say, water erosion or changes in hydrological conditions will change the structure of soil aggregates, turning them into potential aeolian sand. This means that whether it is viewed from the driving mechanism of environmental background or the degradation mechanism of soil texture, the change in hydrological conditions will be an important reason for the formation of dune landforms in oasis area.

Shrub dunes, which are also referred to as coppice dunes or vegetated dunes, form as a result of basic aeolian processes (Tengberg, 1995) and are usually regarded as good indicators of land degradation and the condition of the environment (e.g., Gile, 1975; Zhu et al., 1981b; Tengberg and Chen, 1998; Wang et al., 2006b, Wang et al., 2008b). As is the case for mobile dunes, the development of shrub dune is closely related to vegetation cover, groundwater levels, and the sediment supply (Zhu et al., 1981b; Nickling and Wolfe, 1994; Parsons et al., 2003). However, many shrub dunes only develop in regions with high levels of wind activity and with groundwater maintained within a certain range (Wang et al., 2008b). In the Hexi Corridor and neighboring areas such as the southern Alashan plateau, field investigations show that the shrub dune development can be divided into several stages (**Figure 8**). 1) During the early stage, the amount of water in rivers decreased slowly, but groundwater levels remained high, so no shrub dunes began to develop. 2) During the origin of the shrub

FIGURE 8 | Formation and evolution of shrub dunes in the Hexi Corridor and neighboring areas (modified after Wang et al. (2008b)).
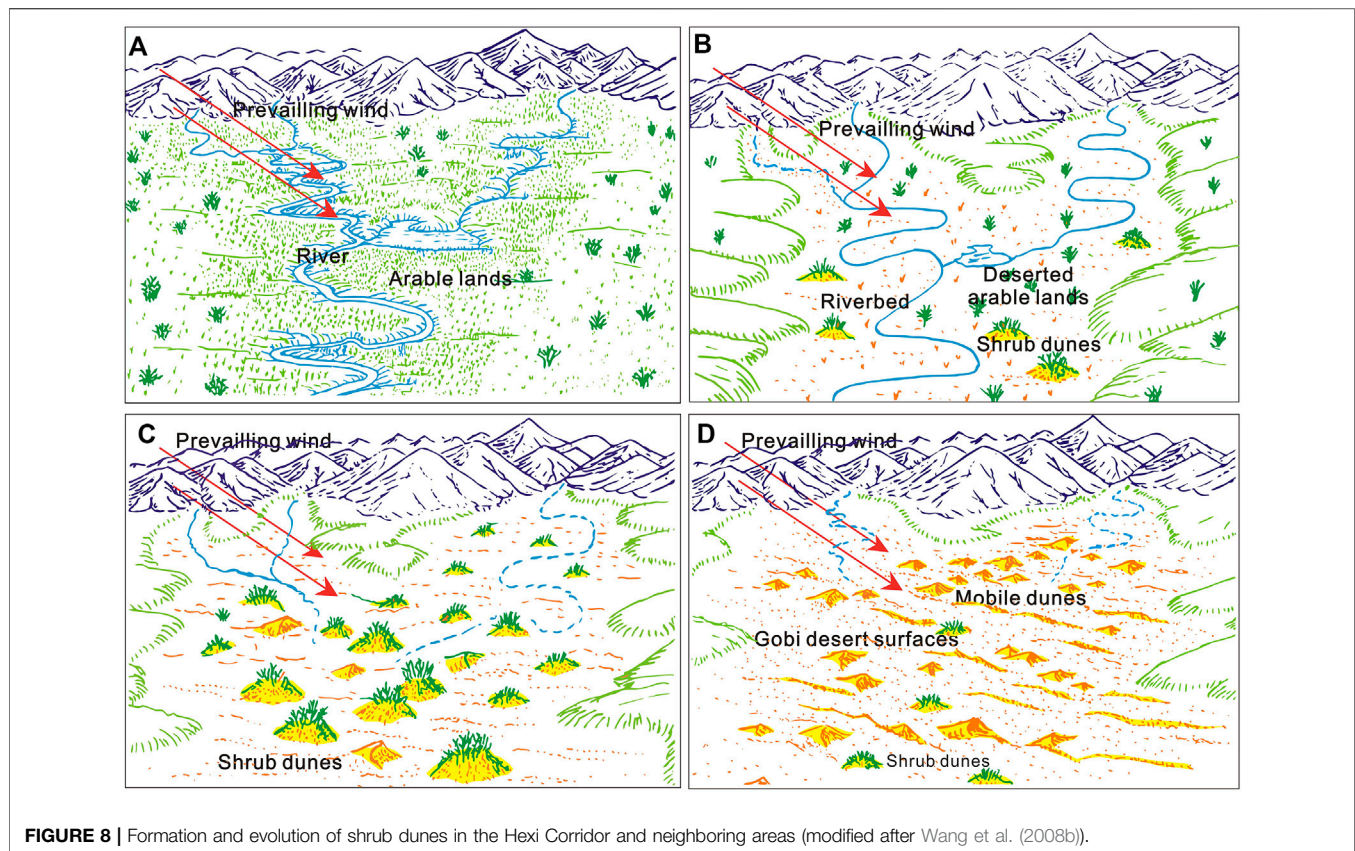
dunes, riverbeds began to emerge due to a decrease in the amount of surface water, and a few shrub dunes began to form on the exposed riverbeds and in deserted arable land. 3) During the developing stage, river beds became thoroughly dry and extensive shrub dune areas began to develop. 4) During the degradation stage, many shrub dunes began to degenerate and evolved into mobile dunes, with only a few distributed in regions with relatively high groundwater levels.

CONCLUSION

Based on comprehensive evidences from geomorphological, aeolian-physical, hydrolgocial, granulometrical and geochemical analysis, this study discussed the dynamical changes of dune landforms and their provenance in the Hexi Corridor. The results show that the dynamic changes of different dunes are different in the Hexi Corridor during the past half century. There are two states of sand dunes movement in the Hexi Corridor in the past half century, dynamic migration and basically stable. This kind of geomorphological evolution of dunes is closely related to their material sources and regional environmental conditions. On the inter-annual and multi-year time scales, the crescent-shaped dunes move the fastest, followed by the chains of barchan dunes. Only the top of the pyramid dunes wigwags, while the parabolic dunes and the longitudinal dunes hardly move forward. The higher the height

of the crescent-shaped dune (or the chain of barchan dunes) is, the slower their movement is. On the contrary, the higher the height of the pyramid dunes is, the faster they swing. Dunes at the edge of the Minqin Oasis move the fastest and dunes at the edge of the Dunhuang Oasis move the slowest. The moving speed of sand dunes in the study area is positively correlated with the average wind speed of local climate and there is a good correlation between the moving speed and the width of dune. The average grain size of sand dunes in the western Hexi Corridor (such as the Huahai-Jinta-Jiaquan area, average 0.27–0.43 mm) is larger than that in the central-eastern Hexi Corridor (such as the Jiuquan-Gaotai-Minqin area, average 0.07–0.24 mm) and also larger than those in other desert regions of northern China (average 0.17–0.19 mm) and of the world (average 0.11–0.23 mm). Different motion modes are identified between aeolian, alluvial/fluvial and gobi sediments. The PC curve of grain size of sand dunes in the Hexi Corridor basically presents a three-stage pattern truncated at about 1.8φ (coarse group) or 2.5φ (fine group), indicating that three modes of motion occur during their transportation. only SiO_2 in the major elements' compositions of dune sands is enriched relative to UCC, most trace elements' abundances are also depleted relative to UCC, except for Cr and Ni. The mineralogical and geochemical data indicate that dune sands in the Hexi Corridor are mainly "sediments of *in-situ* rising" that originated from alluvial/fluvial deposits of ancient rivers, lacustrine deposits of

ancient lakes, and aeolian deposits in the erosion zone of the forelands of the Qilian and Beishan Mountains and the north-neighboring deserts, which means that dried river deposits (playas), alluvial/proluvial deposits, and neighboring desert sands are the main sources of sand dunes in the Hexi Corridor. This reveals that the interaction between wind and water dynamics is of great significance in the formation and evolution of aeolian landforms in terms of geomorphic genesis in arid areas. Sufficient transport capacity is evidenced for both the western and eastern parts of the Hexi Corridor, sufficient sand supply and sand availability, however, is the favorable factor for dune formation in the east part but is the limiting factor for the west.

DATA AVAILABILITY STATEMENT

The original contributions presented in the study are included in the article/Supplementary Materials, further inquiries can be directed to the corresponding author.

REFERENCES

An, F., Zhang, D., Zhao, J., Chai, C., Zhao, Y., and Sun, T. (2019). Physical and Chemical Properties of Soils in Different Types in the Gobi Areas of the Hexi Corridor. *J. Chin. Soil Water Conserv.* 6, 42–47. doi:10.14123/j.cnki.swcc.2019.0143 in Chinese with English abstract

Ashley, G. M. (1978). Interpretation of Polymodal Sediments. *J. Geol.* 86 (4), 411–421. doi:10.1086/649710

Baas, A. C. W., and Nield, J. M. (2007). Modelling Vegetated Dune Landscapes. *Geophys. Res. Lett.* 34, L06405. doi:10.1029/2006GL029152

Bagnold, R. A., and Barndorff-Nielsen, O. (1980). The Pattern of Natural Size Distributions. *Sedimentology* 27, 199–207. doi:10.1111/j.1365-3091.1980.tb01170.x

Bourque, C. P.-A., and Mir, M. A. (2012). Seasonal Snow Cover in the Qilian Mountains of Northwest China: its Dependence on Oasis Seasonal Evolution and lowland Production of Water Vapour. *J. Hydrol.* 454-455, 141–151. doi:10.1016/j.jhydrol.2012.06.008

Bronick, C. J., and Lal, R. (2005). Soil Structure and Management: a Review. *Geoderma* 124, 3–22. doi:10.1016/j.geoderma.2004.03.005

Bureau of Geology and Mineralogy Resources of Gansu Province (BGMRGP) (1984). *Geological Map of Gansu Province of the People's Republic of China 1: 1,000,000.* Beijing, China: Geological Publishing House.

Chang, Z., Li, Y., Zhang, J., Wang, Q., Zhang, D., Tang, J., et al. (2017). Stability Mechanisms of Barchan Sand Dunes: a Case Study in the Hexi Desert in Gansu. *Acta Ecol. Sin.* 37 (13), 4375–4383. doi:10.5846/stxb201602120273 in Chinese with English abstract

Chang, Z. (2019). Problems and Solutions to Desertification Combating in the Hexi, Gansu for 60 Years. *J. Arid Land Resour. Environ.* 33 (9), 152–159. doi:10.13448/j.cnki.jalre.2019.250 in Chinese with English Abstract

Chang, Z., Wang, Q., Zhang, J., Xi, J., Wang, Q., Zhang, D., et al. (2015). Environmental Conditions of Barchans Dune and Barchans Chain – a Case Study from the Hexi Desert Area of Gansu. *Anim. Husbanbandry Feed Sci.* 7 (6), 383–388. doi:10.19578/j.cnki.ahfs.2015.06.017

Chang, Z., Zhu, S., Shi, X., Zhang, J., Li, Y., Wang, Q., et al. (2016). Comparisons between Movement Speed of Main Types of Dunes: a Case Study of Desert Areas in Hexi Region of Gansu Province. *J. Landscape Res.* 8 (6), 36–40. doi:10.16785/j.issn1943-989x.2016.6.010

Chen, F., and Liu, Y. (2011). Secular Annual Movement of Sand Dunes in Badain Jaran Desert Based on Geographic Analyses of Remotely Sensed Imagery. *Remote Sensing Tech. Appl.* 26 (4), 501–507. doi:10.11873/j.issn.1004-0323.2011.4.501

AUTHOR CONTRIBUTIONS

FUNDING

ACKNOWLEDGMENTS

Ci, L., Yang, X., and Chen, Z. (2002). The Potential Impacts of Climate Change Scenarios on Desertification in China. *Earth Sci. Front.* 9, 287–294. in Chinese with English abstract

Ci, L., and Yang, X. (2004). Progress in Feedback Mechanism between Desertification and Climate Change. *Acta Ecol. Sin.* 24, 755–760. in Chinese with English abstract.

Dong, Y., and Huang, D. (2013). Preliminary Observation of Movement of Coastal Dunes in Feicui Island in Changli, Hebei Province. *J. Desert Res.* 33 (2), 486–492. doi:10.7522/j.issn.1000-694X.2013.00066

Dong, Z., Chen, G., Yan, C., Han, Z., and Wang, X. (1998). Movement Laws of Dunes along Oiltransportation Highway in the Tarim Desert. *J. Desert Res.* 18 (4), 328–333. in Chinese with English abstract.

Dong, Z., Su, Z., and Qian, G. (2011). *Aeolian Landforms in the Kumtag Desert.* Beijing: Science Press.

Feng, J.-L., Hu, Z.-G., Ju, J.-T., and Zhu, L.-P. (2011). Variations in Trace Element (Including Rare Earth Element) Concentrations with Grain Sizes in Loess and Their Implications for Tracing the Provenance of Eolian Deposits. *Quat. Int.* 236, 116–126. doi:10.1016/j.quaint.2010.04.024

Ferrat, M., Weiss, D. J., Strekopytov, S., Dong, S., Chen, H., Najorka, J., et al. (2011). Improved Provenance Tracing of Asian Dust Sources Using Rare Earth Elements and Selected Trace Elements for Palaeomonsoon Studies on the Eastern Tibetan Plateau. *Geochim. Cosmochim. Acta* 75, 6374–6399. doi:10.1016/j.gca.2011.08.025

Folk, R. L., and Ward, W. C. (1957). Brazos River Bar [Texas]; a Study in the Significance of Grain Size Parameters. *J. Sediment. Res.* 27, 3–26. doi:10.1306/74d70646-2b21-11d7-8648000102c1865d

Friedman, G. M. (1961). Distinction between Dune, beach, and River Sands from Their Textural Characteristics. *J. Sediment. Pet.* 31 (4), 514–529. doi:10.1306/74d70bcd-2b21-11d7-8648000102c1865d

Gile, L. H. (1975). Holocene Soils and Soil-Geomorphic Relations in an Arid Region of Southern New Mexico. *Quat. Res.* 5, 321–360. doi:10.1016/0033-5894(75)90037-x

Goudie, A. (2002). *Great Warm Deserts of the World: Landscapes and Evolution.* New York: Oxford University Press.

Guan, Q., Zhang, J., Wang, L., Pan, B., Gui, H., and Zhang, C. (2013). Discussion of the Relationship between Dustfall Grain Size and the Desert Border, Taking the Southern Border of the Tengger Desert and the Southern Dust deposit Area as an Example. *Palaeogeogr. Palaeoclimatol. Palaeoecol.* 386, 1–7. doi:10.1016/j.palaeo.2013.01.017

Han, Z. (2003). The Evolution of the Mao Wusu Desert and the Reclamation in the Adjacent Areas in the Ming Dynasty. *China Soc. Sci.* 5, 191–204. in Chinese with English abstract.

Hartmann, K., and Wünnemann, B. (2009). Hydrological Changes and Holocene Climate Variations in NW China, Inferred from lake Sediments of Juyanze Palaeolake by Factor Analyses. *Quat. Int.* 194, 28–44. doi:10.1016/j.quaint.2007.06.037

He, J., Guo, J., Xing, E., Cui, W., and Li, J. (2012). Structure of Wind-Sand Flow and Movement Laws of Dunes along the Yellow River in Ulan Buh Desert. *Trans. Chin. Soc. Agric. Eng.* 28 (17), 71–77. in Chinese with English abstract.

Hetzel, R., Niedermann, S., Tao, M., Kubik, P. W., Ivy-Ochs, S., Gao, B., et al. (2002). Low Slip Rates and Long-Term Preservation of Geomorphic Features in central Asia. *Nature* 417 (6887), 428–432. doi:10.1038/417428a

Hetzel, R., Tao, M., Niedermann, S., Strecker, M. R., Ivy-Ochs, S., Kubik, P. W., et al. (2004). Implications of the Fault Scaling Law for the Growth of Topography: Mountain Ranges in the Broken Foreland of north-east Tibet. *Terra Nova* 16 (3), 157–162. doi:10.1111/j.1365-3121.2004.00549.x

Honda, M., and Shimizu, H. (1998). Geochemical, Mineralogical and Sedimentological Studies on the Taklimakan Desert Sands. *Sedimentology* 45, 1125–1143. doi:10.1046/j.1365-3091.1998.00202.x

Hu, F., Zhang, K., An, Z., and Yu, Y. (2020). Composition of Wind Dynamic Environment Among Desert, Oasis and Gobi. *J. Desert Res.* 40 (4), 113–119. doi:10.7522/j.issn.1000-694X.2020.00034 in Chinese with English abstract

Hu, X., Wang, M., and Liu, Y. (2016). Analysis of Movement of Dunes in the Tengger Desert Based on High-Resolution Remote Sensing Images. *China Sci. Tech. Rev.* 2, 337.

Hugenholtz, C. H., and Wolfe, S. A. (2010). Rates and Environmental Controls of Aeolian Dust Accumulation, Athabasca River Valley, Canadian Rocky Mountains. *Geomorphology* 121, 274–282. doi:10.1016/j.geomorph.2010.04.024

Jahn, B.-M., Gallet, S., and Han, J. (2001). Geochemistry of the Xining, Xifeng and Jixian Sections, Loess Plateau of China: Eolian Dust Provenance and Paleosol Evolution during the Last 140 Ka. *Chem. Geol.* 178, 71–94. doi:10.1016/s0009-2541(00)00430-7

Jiang, Q., and Yang, X. (2019). Sedimentological and Geochemical Composition of Aeolian Sediments in the Taklamakan Desert: Implications for Provenance and Sediment Supply Mechanisms. *J. Geophys. Res. Earth Surf.* 124, 1217–1237. doi:10.1029/2018jf004990

Kimura, R., Bai, L., and Wang, J. (2009). Relationships Among Dust Outbreaks, Vegetation Cover, and Surface Soil Water Content on the Loess Plateau of China, 1999-2000. *Catena* 77, 292–296. doi:10.1016/j.catena.2009.02.016

Kocurek, G., and Lancaster, N. (1999). Aeolian System Sediment State: Theory and Mojave Desert Kelso Dune Field Example. *Sedimentology* 46 (3), 505–515. doi:10.1046/j.1365-3091.1999.00227.x

Küster, Y., Hetzel, R., Krbetschek, M., and Tao, M. (2006). Holocene Loess Sedimentation along the Qilian Shan (China): Significance for Understanding the Processes and Timing of Loess Deposition. *Quat. Sci. Rev.* 25, 114–125. doi:10.1016/j.quascirev.2005.03.003

Lancaster, N. (1995). *Geomorphology of Desert Dunes.* London: Routledge.

Lancaster, N., Wolfe, S., Thomas, D., Bristow, C., Bubenzer, O., Burrough, S., et al. (2016). The INQUA Dunes Atlas Chronologic Database. *Quat. Int.* 410, 3–10. doi:10.1016/j.quaint.2015.10.044

Lancaster, N., Yang, X., and Thomas, D. (2013). Spatial and Temporal Complexity in Quaternary Desert Datasets: Implications for Interpreting Past Dryland Dynamics and Understanding Potential Future Changes. *Quat. Sci. Rev.* 78, 301–302. doi:10.1016/j.quascirev.2013.07.018

Lang, L., Wang, X., Zhu, B., Wang, X., Hua, T., Wang, G., et al. (2017). Nebkha Formation and Variations in Sediment Availability and Wind-Energy Regime of the Western Hexi Corridor over the Past Several Dacades. *J. Desert Res.* 37 (4), 611–620. doi:10.7522/j.isnn.1000-694X.2017.00022 in Chinese with English abstract

Le, B. Y. (1996). Aggregate Stability and Assessment of Soil Crusting and Erodibility: I. Theory and Methodology. *Eur. J. Soil Sci.* 47, 425–437.

Lehmkuhl, F. (1997). The Spatial Distribution of Loess and Loess-like Sediments in the Mountain Areas of central and High Asia. *Z. Geomorphol.* 111, 97–116.

Li, E. (2011). Comparative Study on Characteristics of Aeolian Sediments between the Badanjilin and Tengeli Deserts. Ph.D doctoral dissertation. Xi'an: Shaanxi Normal University). in Chinese with English abstract.

Li, X.-G., Li, F.-M., Rengel, Z., Singh, B., and Wang, Z.-F. (2006). Cultivation Effects on Temporal Changes of Organic Carbon and Aggregate Stability in Desert Soils of Hexi Corridor Region in China. *Soil Tillage Res.* 91, 22–29. doi:10.1016/j.still.2005.10.004

Li, X. G. (2000). The Characteristics of Soil Aggregate in Jintai Electricirrigating Area of Gansu. *Acta Pedol. Sin.* 37, 263–269.

Li, Y., and Zhang, S. (2007). Review of the Research on the Relationship between Sand-Dust Storm and Arid in China. *Adv. Earth Sci.* 22 (11), 1169–1176. in Chinese with English abstract.

Li, Z., Zhang, Z., Wang, M., Nie, H., and Yue, L. (2002). Geological Views on the sandy Desertification of the East Part of north China. *Northwest. Geol.* 35, 7–22. in Chinese with English abstract.

Liu, L., Zhou, J., and Liu, D. (1998). Ivanov IV, Gemkin VA, Prikodko VY. Grassland Soil Changes under Different Uses in the Agro-Pastoral Transitional Zones of north China. *Soils* 5, 225–229.

Liu, T. (1985). *Loess and the Environment.* Beijing: China Ocean Press. in Chinese.

Lu, H., van Huissteden, K., Zhou, J., Vandenberghe, J., Liu, X., and An, Z. (2000). Variability of East Asian Winter Monsoon in Quaternary Climatic Extremes in North China. *Quat. Res.* 54, 321–327. doi:10.1006/qres.2000.2173

Lv, P., Dong, Z., and Rozier, O. (2018). The Combined Effect of Sediment Availability and Wind Regime on the Morphology of Aeolian Sand Dunes. *J. Geophys. Res. Earth Surf.* 123, 2878–2886. doi:10.1029/2017jf004361

Mao, D., Lei, J., Zhou, J., Xue, J., wang, C., and Rehemutula, Z. (2016). Movement Rules of Different Shifting Dunes and Semi-shifting Dunes in Cele, Xinjiang Uygur Autonomous Region. *Res. Soil Water Conser.* 23 (3), 278–282.

Mason, J. A., Nater, E. A., Zanner, C. W., and Bell, J. C. (1999). A New Model of Topographic Effects on the Distribution of Loess. *Geomorphology* 28, 223–236. doi:10.1016/s0169-555x(98)00112-3

McLaren, P., and Bowles, D. (1985). The Effect of Sediment Transport on Size Distributions. *J. Sediment. Pet.* 55 (4), 457–470.

Meyer, B., Tapponnier, P., Bourjot, L., Métivier, F., Gaudemer, Y., Peltzer, G., et al. (1998). Crustal Thickening in Gansu-Qinghai, Lithospheric Mantle Subduction, and Oblique, Strike-Slip Controlled Growth of the Tibet Plateau. *Geophys. J. Int.* 135 (1), 1–47. doi:10.1046/j.1365-246x.1998.00567.x

Minqin Desert Control Experiment Station (MDCES) (1975). *Deserts and Control in Gansu.* Lanzhou: Gansu People's Publishing house, 33–38.

Muhs, D., Bush, C., Cowherd, S., and Mahan, S. (1995). "Geomorphic and Geochemical Evidence for the Source of Sand in the Algodones Dunes, Colorado Desert, southeastern California," in *Desert Aeolian Processes.* Editor V. Tchakerian (London: Chapman & Hall), 37–74.

Muhs, D. R. (2004). Mineralogical Maturity in Dunefields of North America, Africa and Australia. *Geomorphology* 59, 247–269. doi:10.1016/j.geomorph.2003.07.020

Muhs, D. R., Stafford, T. W., Cowherd, S. D., Mahan, S. A., Kihl, R., Maat, P. B., et al. (1996). Origin of the Late Quaternary Dune fields of Northeastern Colorado. *Geomorphology* 17, 129–149. doi:10.1016/0169-555x(95)00100-j

Nickling, W. G., and Wolfe, S. A. (1994). The Morphology and Origin of Nabkhas, Region of Mopti, Mali, West Africa. *J. Arid Environ.* 28, 13–30. doi:10.1016/s0140-1963(05)80017-5

Nottebaum, V., Lehmkuhl, F., Stauch, G., Hartmann, K., Wünnemann, B., Schimpf, S., et al. (2014). Regional Grain Size Variations in Aeolian Sediments along the Transition between Tibetan highlands and north-western Chinese Deserts - the Influence of Geomorphological Settings on Aeolian Transport Pathways. *Earth Surf. Process. Landforms* 39, 1960–1978. doi:10.1002/esp.3590

Nottebaum, V., Lehmkuhl, F., Stauch, G., Lu, H., and Yi, S. (2015a). Late Quaternary Aeolian Sand Deposition Sustained by Fluvial Reworking and Sediment Supply in the Hexi Corridor - an Example from Northern Chinese Drylands. *Geomorphology* 250, 113–127. doi:10.1016/j.geomorph.2015.08.014

Nottebaum, V., Stauch, G., Hartmann, K., Zhang, J., and Lehmkuhl, F. (2015b). Unmixed Loess Grain Size Populations along the Northern Qilian Shan (China): Relationships between Geomorphologic, Sedimentologic and Climatic Controls. *Quat. Int.* 372, 151–166. doi:10.1016/j.quaint.2014.12.071

Pan, K., Zhang, Z., Dong, Z., Zhang, C., and Li, X. (2019). Physicochemical Characteristics of Surface Sediments of crescent-shaped Sand Dunes in the Hexi Corridor, Gansu, China. *J. Desert Res.* 39 (1), 44–51. doi:10.7522/j.issn.1000-694X.2018.00150 in Chinese with English abstract

Parsons, A. J., Wainwright, J., Schlesinger, W. H., and Abrahams, A. D. (2003). The Role of Overland Flow in Sediment and Nitrogen Budgets of mesquite Dunefields, Southern New Mexico. *J. Arid Environ.* 53, 61–71. doi:10.1006/jare.2002.1021

Pease, P. P., and Tchakerian, V. P. (2003). Geochemistry of Sediments from Quaternary Sand Ramps in the southeastern Mojave Desert, California. *Quat. Int.* 104, 19–29. doi:10.1016/s1040-6182(02)00132-5

Pease, P. P., Tchakerian, V. P., and Tindale, N. W. (1998). Aerosols over the Arabian Sea: Geochemistry and Source Areas for Aeolian Desert Dust. *J. Arid Environ.* 39, 477–496. doi:10.1006/jare.1997.0368

Pettijohn, F. J., Potter, P. E., and Siever, R. (1972). *Sand and Sandstone*. New York: Springer-Verlag.

Prins, M. A., and Vriend, M. (2007). Glacial and Interglacial Eolian Dust Dispersal Patterns across the Chinese Loess Plateau Inferred from Decomposed Loess Grain-Size Records. *Geochem. Geophys. Geosys.* 8 (7), Q07Q05. doi:10.1029/2006gc001563

Pu, Z. (2005). For the Lost Oasis - a Review of Studies on Desertification in the Hexi Corridor during the Historical Period. *Collections Essays Chin. Hist. Geogr.* 20 (1), 157–158. in Chinese.

Pye, K. (1995). The Nature, Origin and Accumulation of Loess. *Quat. Sci. Rev.* 14, 653–667. doi:10.1016/0277-3791(95)00047-x

Qiang, M., Chen, F., Zhou, A., Xiao, S., Zhang, J., and Wang, Z. (2007). Impacts of Wind Velocity on Sand and Dust Deposition during Dust Storm as Inferred from a Series of Observations in the Northeastern Qinghai-Tibetan Plateau, China. *Powder Tech.* 175 (2), 82–89. doi:10.1016/j.powtec.2006.12.020

Qiang, M., Lang, L., and Wang, Z. (2010). Do fine-grained Components of Loess Indicate Westerlies: Insights from Observations of Dust Storm Deposits at Lenghu (Qaidam Basin, China). *J. Arid Environ.* 74 (10), 1232–1239. doi:10.1016/j.jaridenv.2010.06.002

Qu, J., Huang, N., Ta, W., Lei, J., and Dong, Z. (2005). Structural Characteristics of Gobi Sanddrift and its Significance. *Adv. Earth Sci.* 20 (1), 19–23. in Chinese with English abstract.

Ren, X. (2010). Element Analysis of Surface Sediments from Active Dunes in the Minqin Oasis and its Adjacent Deserts. Ma.D Dissertation. Lanzhou: Lanzhou University. in Chinese with English abstract.

Ren, X., Liu, T., and Wang, Z. (2010). Characters of Geomorphologic Parameter about Barchans Dunes. *Res. Soil Water Conser.* 17 (1), 163–166. in Chinese with English abstract.

Ren, X., and Wang, Z. (2010). The Provenance of Eolian Sediments in Minqin Oasis, Gansu Province. *J. Ningxia Univ. Nat. Sci. Edition* 31 (1), 88–92. in Chinese with English abstract.

Ren, X., Yang, X., Wang, Z., Zhu, B., Zhang, D., and Rioual, P. (2014). Geochemical Evidence of the Sources of Aeolian Sands and Their Transport Pathways in the Minqin Oasis, Northwestern China. *Quat. Int.* 334-335, 165–178. doi:10.1016/j.quaint.2014.04.037

Rubin, D. M., and Hesp, P. A. (2009). Multiple Origins of Linear Dunes on Earth and Titan. *Nat. Geosci.* 2 (9), 653–658. doi:10.1038/ngeo610

Runnström, M. C. (2003). Rangeland Development of the Mu Us sandy Land in Semiarid China: an Analysis Using Landsat and NOAA Remote Sensing Data. *Land Degrad. Dev.* 14, 189–202. doi:10.1002/ldr.545

Sahu, B. K. (1964). Depositional Mechanisms from the Size Analysis of Clastic Sediments. *J. Sediment. Res.* 34 (1), 73–83. doi:10.1306/74d70fce-2b21-11d7-8648000102c1865d

Schettler, G., Romer, R. L., Qiang, M., Plessen, B., and Dulski, P. (2009). Size-dependent Geochemical Signatures of Holocene Loess Deposits from the Hexi Corridor (China). *J. Asian Earth Sci.* 35 (2), 103–136. doi:10.1016/j.jseaes.2009.01.003

Shi, X., Li, G., Liu, S., and Wei, Y. (2018). Dynamic Changes of Barchans Dunes and its Relationship with Meteorological Factors along Oasis Fringe in Hexi Corridor. *J. Gansu Agric. Univ.* 2, 86–93. In Chinese with English Abstract.

Stauch, G., IJmker, J., Pötsch, S., Zhao, H., Hilgers, A., Diekmann, B., et al. (2012). Aeolian Sediments on the north-eastern Tibetan Plateau. *Quat. Sci. Rev.* 57, 71–84. doi:10.1016/j.quascirev.2012.10.001

Stauch, G., Pötsch, S., Zhao, H., and Lehmkuhl, F. (2014). Interaction of Geomorphological Processes on the north-eastern Tibetan Plateau during the Holocene, an Example from a Sub-catchment of Lake Donggi Cona. *Geomorphology* 210, 23–35. doi:10.1016/j.geomorph.2013.12.014

Su, Y.-z., Wang, F., Zhang, Z.-h., and Du, M.-w. (2007). Soil Properties and Characteristics of Soil Aggregate in Marginal Farmlands of Oasis in the Middle of Hexi Corridor Region, Northwest China. *Agric. Sci. China* 6 (6), 706–714. doi:10.1016/s1671-2927(07)60103-5

Su, Y. (2007). Soil Carbon and Nitrogen Sequestration Following the Conversion of Cropland to Alfalfa Forage Land in Northwest China. *Soil Tillage Res.* 92, 181–189. doi:10.1016/j.still.2006.03.001

Sun, D., Bloemendal, J., Rea, D. K., Vandenberghe, J., Jiang, F., An, Z., et al. (2002). Grain Size Distribution Function of Polymodal Sediments in Hydraulic and Aeolian Environments and Numerical Partitioning of the Sedimentary Components. *Sediment. Geol.* 152 (3-4), 263–277. doi:10.1016/s0037-0738(02)00082-9

Sun, D., Chen, F., Bloemendal, J., and Su, R. (2003). Seasonal Variability of Modern Dust over the Loess Plateau of China. *J. Geophys. Res. Atmos.* 108 (D21), 4665. doi:10.1029/2003jd003382

Sun, J. (2002). Provenance of Loess Material and Formation of Loess Deposits on the Chinese Loess Plateau. *Earth Planet. Sci. Lett.* 203, 845–859. doi:10.1016/s0012-821x(02)00921-4

Sun, W., and Li, B. (2002). The Relation between Coupling Among the Principal Components of Desertification Factors and Desertification in Rear hills of Bashang since 1950. *Geogr. Res.* 21, 392–397. in Chinese with English abstract.

Sun, W. (2000). News & Notes. *Seismol. Res. Lett.* 71, 154–158. in Chinese with English abstract. doi:10.1785/gssrl.71.2.154

Ta, W., Xiao, H., Qu, J., Xiao, Z., Yang, G., Wang, T., et al. (2004). Measurements of Dust Deposition in Gansu Province, China, 1986-2000. *Geomorphology* 57, 41–51. doi:10.1016/s0169-555x(03)00082-5

Tapponnier, P., Meyer, B., Avouac, J. P., Peltzer, G., Gaudemer, Y., Guo, S., et al. (1990). Active Thrusting and Folding in the Qilian Shan, and Decoupling between Upper Crust and Mantle in Northeastern Tibet. *Earth Planet. Sci. Lett.* 97, 387–403. doi:10.1016/0012-821x(90)90053-z

Taylor, S. R., and McLennan, S. M. (1985). *The Continental Crust: Its Composition and Evolution*. London: Blackwell Scientific Publications.

Tengberg, A., and Chen, D. (1998). A Comparative Analysis of Nebkhas in central Tunisia and Northern Burkina Faso. *Geomorphology* 22, 181–192. doi:10.1016/s0169-555x(97)00068-8

Tengberg, A. (1995). Nebkha Dunes as Indicators of Wind Erosion and Land Degradation in the Sahel Zone of Burkina Faso. *J. Arid Environ.* 30, 265–282. doi:10.1016/s0140-1963(05)80002-3

Thomas, D. S. G., Knight, M., and Wiggs, G. F. S. (2005). Remobilization of Southern African Desert Dune Systems by Twenty-First century Global Warming. *Nature* 435, 1218–1221. doi:10.1038/nature03717

Thomas, D. S. G., and Leason, H. C. (2005). Dunefield Activity Response to Climate Variability in the Southwest Kalahari. *Geomorphology* 64, 117–132. doi:10.1016/j.geomorph.2004.06.004

Vandenberghe, J. (2013). Grain Size of fine-grained Windblown Sediment: a Powerful Proxy for Process Identification. *Earth Sci. Rev.* 121, 18–30. doi:10.1016/j.earscirev.2013.03.001

Visher, G. (1969). Grain Size Distributions and Depositional Processes. *J. Sediment. Res.* 39 (3), 1074–1106. doi:10.1306/74d71d9d-2b21-11d7-8648000102c1865d

Wang, G., Cheng, G., and Du, M. (2003c). "The Impacts of Human Activity on Hydrological Processes in the Arid Zones of the Hexi Corridor, Northwest China, in the Past 50 Years," in *Water Resources Systems - Water Availability and Global Change*. Editor S. Franks (Oxfordshire Wallingford: IAHS Publisher), 280, 93–103.

Wang, J., Li, W., Song, D., Tang, H., and Dong, G. (2004). The Analysis of Land Desertification Changing of Minqin County in Recent 30 Years. *J. Remote Sensing* 8, 282–288.

Wang, J., Liu, L., and Shen, L. (2013a). Research of Movement Laws of Barchan Dunes in the Mu Us sandy Land Based on Google Earth Software. *Remote Sensing Tech. Appl.* 28 (6), 1094–1100.

Wang, L. (2011). Surface Deposits in the Hexi Corridor and its Adjacent Areas and Implications for Provenance of Asian Dust. Ma.D Dissertation. Lanzhou: Lanzhou University. in Chinese with English abstract.

Wang, L., and Wang, Q. (2013). Elemental Compositions of Surface Deposits in the Hexi Corridor and its Adjacent Areas, Northwestern China. *Northwest. Geol.* 46 (2), 69–80. in Chinese with English abstract.

Wang, N., Zhao, Q., Hu, G., and Chen, Y. (2003a). Climatic and Humanistic Background of Desertification Process in the Recent 2000 Years in Hexi Corridor, China. *J. Desert Res.* 23, 95–100. in Chinese with English abstract.

Wang, N. A., Li, Z., Li, Y., and Cheng, H. (2013b). Millennial-scale Environmental Changes in the Asian Monsoon Margin during the Holocene, Implicated by the lake Evolution of Huahai Lake in the

Hexi Corridor of Northwest China. *Quat. Int.* 313-314, 100–109. doi:10.1016/j.quaint.2013.08.039

Wang, T. (2003). *Desert and Desertification in China*. Shijiazhuang: Hebei Science and Technology Press. in Chinese.

Wang, T., Wu, W., Xue, X., Han, Z., Zhang, W., and Sun, Q. (2004a). Spatial–temporal Changes of sandy Desertified Land during Last 5 Decades in Northern China. *Acta Geogr. Sin.* 59, 203–212. in Chinese with English abstract.

Wang, T., Wu, W., Xue, X., Zhang, W., Han, Z., and Sun, Q. (2003b). Time–space Evolution of Desertification Land in Northern China. *J. Desert Res.* 23, 230–235. in Chinese with English abstract.

Wang, T., Wu, W., Zhao, H., Hu, M., and Zhao, A. (2004b). Analyses on Driving Factors to sandy Desertification Process in Horqin Region, China. *J. Desert Res.* 24, 519–528. in Chinese with English abstract.

Wang, W. (2002). When Maowusu Became a Desert? - View through New Archaeological Finds. *Archaeol. Cult. Relics* 5, 80–85. in Chinese with English abstract.

Wang, X., Lang, L., Hua, T., Zhang, C., and Wang, Z. (2013c). Gravel Cover of Gobi Desert and its Significance for Wind Erosion: an Experimental Study. *J. Desert Res.* 33 (2), 313–319. doi:10.7522/j.issn.1000-694X.2013.00044 in Chinese with English abstract

Wang, X., Chen, F.-H., Dong, Z., and Xia, D. (2005). Evolution of the Southern Mu Us Desert in North China over the Past 50 years: an Analysis Using Proxies of Human Activity and Climate Parameters. *Land Degrad. Dev.* 16, 351–366. doi:10.1002/ldr.663

Wang, X., Chen, F., and Dong, Z. (2006a). The Relative Role of Climatic and Human Factors in Desertification in Semiarid China. *Glob. Environ. Change* 16, 48–57. doi:10.1016/j.gloenvcha.2005.06.006

Wang, X., Chen, F., Hasi, E., and Li, J. (2008a). Desertification in China: an Assessment. *Earth Sci. Rev.* 88, 188–206. doi:10.1016/j.earscirev.2008.02.001

Wang, X., Hua, T., Zhu, B., Lang, L., and Zhang, C. (2018). Geochemical Characteristics of the fine-grained Component of Surficial Deposits from Dust Source Areas in Northwestern China. *Aeolian Res.* 34, 18–26. doi:10.1016/j.aeolia.2018.07.004

Wang, X., Huang, N., Dong, Z., and Zhang, C. (2010). Mineral and Trace Element Analysis in Dustfall Collected in the Hexi Corridor and its Significance as an Indicator of Environmental Changes. *Environ. Earth Sci.* 60, 1–10. doi:10.1007/s12665-009-0164-8

Wang, X., Wang, T., Dong, Z., Liu, X., and Qian, G. (2006b). Nebkha Development and its Significance to Wind Erosion and Land Degradation in Semi-arid Northern China. *J. Arid Environ.* 65, 129–141. doi:10.1016/j.jaridenv.2005.06.030

Wang, X., Xiao, H., Li, J., Qiang, M., and Su, Z. (2008b). Nebkha Development and its Relationship to Environmental Change in the Alaxa Plateau, China. *Environ. Geol.* 56, 359–365. doi:10.1007/s00254-007-1171-2

Ward, J. H. (1963). Hierarchical Grouping to Optimize an Objective Function. *J. Am. Stat. Assoc.* 58, 236–244. doi:10.1080/01621459.1963.10500845

Wasson, R. J., and Hyde, R. (1983). Factors Determining Desert Dune Type. *Nature* 304 (5924), 337–339. doi:10.1038/304337a0

Weltje, G. J., and Prins, M. A. (2007). Genetically Meaningful Decomposition of Grain-Size Distributions. *Sediment. Geol.* 202 (3), 409–424. doi:10.1016/j.sedgeo.2007.03.007

Williams, M. (2014). *Climate Change in Deserts: Past, Present and Future*. New York: Cambridge University Press.

Wolfe, S. A., R. Muhs, D., David, P. P., and McGeehin, J. P. (2000). Chronology and Geochemistry of Late Holocene Eolian Deposits in the Brandon Sand Hills, Manitoba, Canada. *Quat. Int.* 67, 61–74. doi:10.1016/s1040-6182(00)00009-4

Wolff, D. D., and Parsons, M. L. (1983). *Pattern Recognition Approach to Data Interpretation*. New York: Pienum Press.

Wu, B., and Ci, L. (1998). Causes and Development Stages of Desertification in the Mu Us Sandland. *Chin. Sci. Bull.* 43, 2437–2440. in Chinese.

Wu, B., and Ci, L. J. (2002). Landscape Change and Desertification Development in the Mu Us Sandland, Northern China. *J. Arid Environ.* 50, 429–444. doi:10.1006/jare.2001.0847

Wu, W. (2001). Study on Processes of Desertification in Mu Us Sandy Land for Last 50 years, China. *J. Desert Res.* 21, 164–169. in Chinese with English abstract.

Wu, W., Wang, X., and Yao, F. (1997). Applying Remote Sensing Data for Desertification Monitoring in the Mu Us Sandy Land. *J. Desert Res.* 17, 415–420. in Chinese with English abstract.

Yang, T. (1985). Land Desertification on the Fringe Area of Inner Mongolia Plateau Adjacent to Heibei Province and its Rehabilitation. *J. Desert Res.* 5 (4), 25–35. in Chinese with English abstract.

Yang, X., Liang, P., Zhang, D., Li, H., Rioual, P., Wang, X., et al. (2019). Holocene Aeolian Stratigraphic Sequences in the Eastern Portion of the Desert belt (Sand Seas and sandy Lands) in Northern China and Their Palaeoenvironmental Implications. *Sci. China Earth Sci.* 62, 1302–1315. doi:10.1007/s11430-018-9304-y

Yang, X. (2006). Desert Research in Northwestern China. A Brief Review. *Geomorphologie* 12, 275–284. doi:10.4000/geomorphologie.79

Yang, X., Li, H., and Conacher, A. (2012). Large-scale Controls on the Development of Sand Seas in Northern China. *Quat. Int.* 250, 74–83. doi:10.1016/j.quaint.2011.03.052

Yang, X., Rost, K. T., Lehmkuhl, F., Zhenda, Z., and Dodson, J. (2004). The Evolution of Dry Lands in Northern China and in the Republic of Mongolia since the Last Glacial Maximum. *Quat. Int.* 118-119, 69–85. doi:10.1016/s1040-6182(03)00131-9

Yang, X., Scuderi, L., Paillou, P., Liu, Z., Li, H., and Ren, X. (2011). Quaternary Environmental Changes in the Drylands of China - A Critical Review. *Quat. Sci. Rev.* 30, 3219–3233. doi:10.1016/j.quascirev.2011.08.009

Yang, X., Zhu, B., Wang, X., Li, C., Zhou, Z., Chen, J., et al. (2008). Late Quaternary Environmental Changes and Organic Carbon Density in the Hunshandake Sandy Land, Eastern Inner Mongolia, China. *Glob. Planet. Change* 61, 70–78. doi:10.1016/j.gloplacha.2007.08.007

Yang, X., Zhu, B., and White, P. D. (2007). Provenance of Aeolian Sediment in the Taklamakan Desert of Western China, Inferred from REE and Major-Elemental Data. *Quat. Int.* 175, 71–85. doi:10.1016/j.quaint.2007.03.005

Yin, D., Qu, J., Zhao, S., Tan, L., An, Z., and Xiao, J. (2016). Amount Of Wind Erosion To Gravel Gobi Under Different Disturbing Modes. *Arid Land Geo.* 39 (3), 495–503.

Yin, D., Qu, J., Zu, R., Tan, L., and An, Z. (2014). Impact of Disturbing on Amount of Wind Erosion of sandy Gobi. *J. Desert Res.* 34 (1), 1–8. doi:10.7522/j.issn.1000-694X.2013.00279 in Chinese with English abstract

Zhang, K., Qu, J., Zu, R., and Fang, H. (2004). Wind Tunnel Simulation about the Effects of the Different Underlying Surfaces on the Features of Drifting Sand Current. *Arid Land Geogr.* 37 (3), 352–355. in Chinese with English abstract.

Zhang, L., and Ren, G. (2003). Change in Dust Storm Frequency and the Climatic Controls in Northern China. *Acta Meteorol. Sin.* 61 (6), 744–750. in Chinese with English abstract.

Zhang, X., Wang, X., and Yan, P. (2008). Re-evaluating the Impacts of Human Activity and Environmental Change on Desertification in the Minqin Oasis, China. *Environ. Geol.* 55, 705–715. doi:10.1007/s00254-007-1022-1

Zhang, Z., and Dong, Z. (2014). Dune Field Patterns and Wind Environments in the Middle Reaches of the Heihe Basin. *J. Desert Res.* 34 (2), 332–341. doi:10.7522/j.issn.1000-694X.2013.00323 in Chinese with English abstract

Zhang, Z., and Dong, Z. (2015). Grain Size Characteristics in the Hexi Corridor Desert. *Aeolian Res.* 18, 55–67. doi:10.1016/j.aeolia.2015.05.006

Zhang, Z., Dong, Z., Li, J., Qian, G., and Jiang, C. (2016). Implications of Surface Properties for Dust Emission from Gravel Deserts (Gobis) in the Hexi Corridor. *Geoderma* 268, 69–77. doi:10.1016/j.geoderma.2016.01.011

Zhang, Z., Dong, Z., Zhang, C., Qian, G., and Lei, C. (2017). The Geochemical Characteristics of Dust Material and Dust Sources Identification in Northwestern China. *J. Geochem. Explor.* 175, 148–155. doi:10.1016/j.gexplo.2016.11.006

Zhang, Z., Pan, K., Zhang, C., and Liang, A. (2020). Geochemical Characteristics and the Provenance of Aeolian Material in the Hexi Corridor Desert, China. *Catena* 190, 104483. doi:10.1016/j.catena.2020.104483

Zhao, Y. (1981). Mu Us Desert Evolution in Historical Periods. *Hist. Geogr.* 1, 34–47. in Chinese.

Zhu, B. (2007). Geochemistry, Hydrochemistry and Sedimentology of the Taklamakan Desert in Tarim Basin, NW China. Ph.D doctoral dissertation. Beijing: Institute of Geology and Geophysics Chinese Academy of Sciences.

Zhu, B.-Q., and Wang, Y.-L. (2016). Statistical Study to Identify the Key Factors Governing Ground Water Recharge in the Watersheds of the Arid Central Asia. *Environ. Monit. Assess.* 188, 66. doi:10.1007/s10661-015-5075-4

Zhu, B.-Q., Yu, J.-J., Rioual, P., and Ren, X.-Z. (2014). Particle Size Variation of Aeolian Dune Deposits in the Lower Reaches of the Heihe River basin, China. *Sediment. Geol.* 301, 54–69. doi:10.1016/j.sedgeo.2013.12.006

Zhu, B., Wang, X., and Rioual, P. (2017). Multivariate Indications between Environment and Ground Water Recharge in a Sedimentary Drainage basin

in Northwestern China. *J. Hydrol.* 549, 92–113. doi:10.1016/j.jhydrol.2017.03.058

Zhu, B., and Yang, X. (2009). Chemical Weathering of Detrital Sediments in the Taklamakan Desert, Northwestern China. *Geogr. Res.* 47 (1), 57–70. doi:10.1111/j.1745-5871.2008.00555.x

Zhu, B., and Yu, J. (2014). Aeolian Sorting Processes in the Ejina Desert basin (China) and Their Response to Depositional Environment. *Aeolian Res.* 12, 111–120. doi:10.1016/j.aeolia.2013.12.004

Zhu, Z., and Chen, G. (1994). *Sandy Desertification in China*. Beijing: Science press. in Chinese.

Zhu, Z., Chen, Z., Wu, Z., Li, J., Li, B., and Wu, G. (1981a). *Study on the Geomorphology of Wind-Drift Sands in the Taklamakan Desert*. Beijing: Science Press. in Chinese.

Zhu, Z. (1999). *Deserts, Desertification, Land Degradation and Strategies for Rehabilitation in China*. Beijing: Environmental Press. in Chinese.

Zhu, Z., Guo, H., and Wu, Q. (1964). Study on the Movement of Dunes Near Oases in the Southwest of the Taklimakan Desert. *Acta Geogr. Sin.* 30 (1), 35–50.

Zhu, Z., Liu, S., and Xiao, L. (1981b). The Characteristics of the Environment Vulnerable to Desertification and the Ways of its Control in Steppe Zone. *J. Desert Res.* 1, 2–12. in Chinese with English abstract.

Zhu, Z. (1985). Status and Trend of Desertification in Northern China. *J. Desert Res.* 5, 3–11. in Chinese with English abstract.

Zhu, Z., and Wang, T. (1992). Theory and Practice on sandy Desertification in China. *Quat. Sci.* 2, 97–106. in Chinese with English abstract.

Zhu, Z., Wu, Z., Liu, S., and Di, X. (1980). *An Outline of Chinese Deserts*. Beijing: Science Press. in Chinese.

Zimbelman, J. R., and Williams, S. H. (2002). Geochemical Indicators of Separate Sources for Eolian Sands in the Eastern Mojave Desert, California, and Western Arizona. *Geol. Soc. Am. Bull.* 114, 490–496. doi:10.1130/0016-7606(2002)114<0490:giossf>2.0.co;2